The Smn-independent beneficial effects of trichostatin A on an intermediate mouse model of spinal muscular atrophy

by
Armin Yazdani

Thesis presented as a partial
requirement for the
Master's of Science (M.Sc.) in Cellular and Molecular Medicine

Department of Cellular and Molecular Medicine
University of Ottawa
Ottawa, Ontario, Canada

Abstract

Trichostatin A (TSA) is a histone deacetylase inhibitor with beneficial effects in spinal muscular atrophy mouse models that carry the human *SMN2* transgene. Whether TSA specifically targets the upregulation of the *SMN2* gene or whether other genes respond to TSA and in turn provide neuroprotection in SMA mice is unclear. We have taken advantage of the $Smn^{2B/-}$ mouse model that does not harbor the human *SMN2* transgene, to test the hypothesis that TSA has its beneficial effects through a non-Smn mediated pathway. Daily intraperitoneal injection of TSA from postnatal day 12 to 25 was performed in the $Smn^{2B/-}$ mice and littermate controls. Previous work from our laboratory demonstrated that treatment with TSA increased the median lifespan of $Smn^{2B/-}$ mice from twenty days to eight weeks. As well, there was a significant attenuation of weight loss and improved motor behavior. Pen test and righting reflex both showed significant improvement, and motor neurons in the spinal cord of $Smn^{2B/-}$mice were protected from degeneration. Both the size and maturity of neuromuscular junctions were significantly improved in TSA treated $Smn^{2B/-}$ mice. Here, we have shown that TSA treatment does not increase the levels of Smn protein in mouse embryonic fibroblasts or myoblasts obtained from the $Smn^{2B/-}$ mice. Further, qPCR analysis revealed no changes in the level of *Smn* transcripts in the brain or spinal cord of TSA-treated SMA mice. Similarly, western blot analysis revealed no significant increase in Smn protein levels in the brain, spinal cord, hind limb muscle, heart muscle, or the liver of TSA treated $Smn^{2B/-}$ mice. However, TSA has beneficial effects in the muscles of $Smn^{2B/-}$ mice and improves motor behavior and myofiber size. TSA improves muscle development by enhancing the activity of myogenic regulatory factors independent of the *Smn* gene. The beneficial

effect of TSA is therefore likely through an Smn-independent manner. Identification of these protective pathways will be of therapeutic value for the treatment of SMA.

Table of Contents

List of tables

List of figures

List of abbreviations

Ac H3; Acetylated Histone H3
Ac H4; Acetylated Histone H4
bp; Base pairs
DMSO; Dimethyl sulfoxide
H3; Total Histone H3
H4; Total Histone H4
HAT; Histone acetyl transferases
HDAC; Histone deacetylase
HDACi; Histone deacetylase inhibitor
hnRNPA1; Heterogeneous nuclear ribonucleoprotein A1
IP; Intraperitoneal
kDa; Kilodalton
MyoG; Myogenin
NAD; Nicotinamide adenine dinucleotide
NMJ; Neuromuscular junction
P; Postnatal day
PAGE; Polyacrylamide gel electrophoresis
Pax7; Paired box protein 7
PBS; Phosphate-buffered saline
qPCR; Quantitative polymerase chain reaction
RhoA; Ras homolog gene family, member A
RNP; Ribonucleoprotein
ROCK; RhoA kinase
RT-PCR; Reverse transcription- polymerase chain reaction
SAHA; Suberoylanilide hydroxamic acid
SDS; Sodium dodecyl sulfate
SF2/ASF; Serine/arginine-rich splicing factor 1/ alternative splicing factor 1
SIRT; Sirtuins
SMA; Spinal muscular atrophy
SMN; Survival motor neuron
SMN2; Survival motor neuron 2
snRNP; Small nuclear ribonucleic particles
TSA; Trichostatin A
VPA; Valproic acid
Wt; Wildtype

Acknowledgements

I would first and foremost like to extend my sincere gratitude to my supervisor and mentor, Dr. Rashmi Kothary, for significant support, patience, advice, and guidance. It has been a tremendous honor to be given the opportunity to learn from such a distinguished and accomplished scientist and generous and humble man. I would like to thank Dr. Lyndsay Murray for her support, mentorship, advice, and technical expertise throughout the project. Additionally, I would like to acknowledge and thank my lab members both past and present for their helpful thoughts and discussions. I would also like to thank my committee members, Dr. Jocelyn Cote and Dr. Jeffery Dilworth, for their support, valuable insights and constructive comments throughout my studies. Last but not least, I would like to thank my family and friends for their generous support and kind encouragement during these past two years.

Introduction

Spinal Muscular Atrophy (SMA) is an autosomal recessive neuromuscular disorder characterized by the progressive loss of alpha motor neurons in the anterior horn region of the spinal cord causing symmetrical weakness and atrophy of proximal voluntary muscles. The spinal muscular atrophies are the second most common autosomal-recessive inherited disorders after cystic fibrosis. In a review by Kolb et al., the original description of SMA was traced to 2 infant brothers by Guido Werdnig from University of Vienna in 1891 and in 7 additional cases by Johan Hoffmann from Heidelberg University (Kolb et al., 2011). Spinal muscular atrophy is a leading cause of infant and childhood mortality and morbidity with a carrier frequency of 1:40-50 and an incidence of between 1 in 6000-10000 (Pearn et al., 1978; Crawford et al., 1996; Sugarman et al., 2012). The timeline of landmark discoveries in SMA are summarized in **Figure 1** (Kolb et al., 2011).

Clinical Subtypes

SMA is clinically divided into five categories based on age of onset, disease severity, and time to reach locomotor milestones (summarized in Table 1). Type 0 SMA has a prenatal onset and is illustrated by reduced fetal movement in utero and death neonataly (Dubowitz et al., 1999). Type 1 SMA (Werdnig-Hoffmann) is the most common form and has a disease onset of 6 months. The majority of type 1 SMA patients

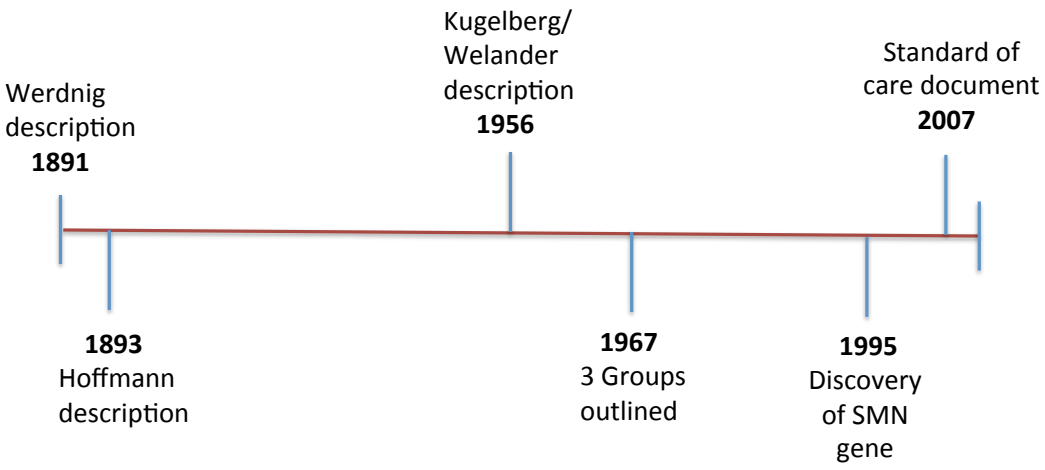

Figure 1. Spinal muscular atrophy (SMA) timeline

The discovery of the gene in 1995 leads to the rapid expansion of research and lead to various therapeutic approaches (Adapted from Kolb et al. 2011).

Type	Age of Onset	Milestone Achieved	Natural Age of Death
Type I	0-6 months	Never sit	< 2 years
Type II	7-18 months	Sit, never stand	> 2 years
Type III	> 18 months	Stand and walk	Adult
Type IV	Second or third decade of life	Walk during adulthood	Adult

Table 1. Disease classification of SMA

SMA can be classified into 4 categories depending on age of onset and disease severity. Type I SMA is the most severe and common form of SMA. Type IV SMA is the adult onset form of the disease and is milder in clinical presentation and disease progression.

have normal strength at birth however start to present with progressive weakness within a few weeks or months. Type 1 SMA patients typically die from respiratory collapse before the age of two, however this can be extended with proper respiratory care and nutritional support (Oskoui et al., 2007). Types 2 and 3 (Kugelberg-Welander) are milder and present between 6 months to 2 years of age initially with delayed progression of motor milestones, however onset could be delayed to a much later age particularly in type 3 patients (Munsat et al., 1992). Type 4 SMA has an adult onset and most patients develop symptoms after the age of 30. Clinically most patients have a variety of symptoms affecting the musculoskeletal system such as weakness in proximal leg, arm, trunk muscles, muscular atrophy, scoliosis, intercostal muscle weakness, which eventually leads to respiratory failure and death. While SMA affects both sexes, males are most frequently afflicted with the early onset forms such as type I and type II SMA (Hausmanowa-Petrusewicz et al., 1984).

Genetic Etiology

The genetic etiology of SMA was established in 1995 when mutations and deletions in a gene located on chromosome 5q13 called Survival of Motor Neuron 1 (*SMN1*) were identified (Lefebvre et al., 1995). The majority of SMA patients have deletions that often span exons 6-8, however a variety of missense mutations and frameshift mutations *(*summarized in **Figure 2**) have been identified and are sufficient to

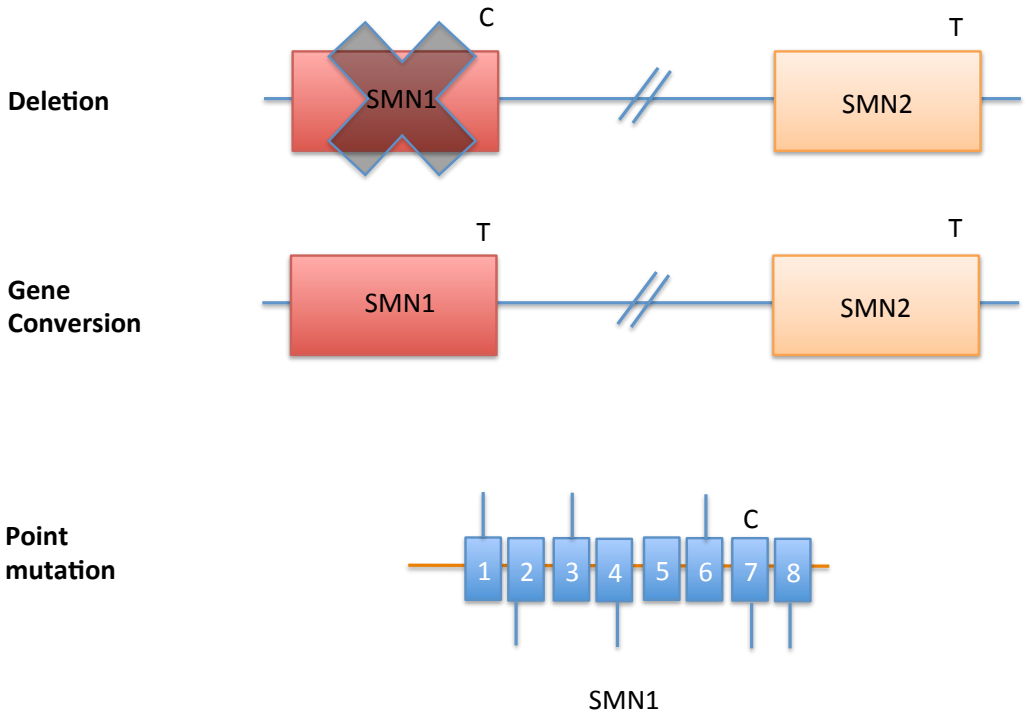

Figure 2. Common mutations observed in *SMN1*

Deletions, gene conversions, and point mutations are the events that render *SMN1* dysfunctional. Deletions remove parts or the entire length of *SMN1* and cause SMA. Gene conversion events are also common and convert *SMN1* to behave like *SMN2*. Point mutations are also observed in *SMN1* but occur at a much lower frequency.

cause SMA (Wirth et al., 2000). The *SMN* gene is highly conserved throughout evolution and all eukaryotic organisms display at least one copy of the gene however humans also carry another copy that is nearly identical (99%), called *SMN2* (Lefebvre et al., 1995; DiDonato et al., 1997). The telomeric copy (*SMN1*) expresses the full-length protein and the centromeric copy (*SMN2*) primarily expresses a truncated form due to a cytidine to thymine substitution in position 6 of exon 7, which is the splice enhancer region critical to exon 7 inclusion (Lorson et al., 1999). This substitution alters the splicing pattern resulting in a transcript lacking exon 7 and consequently yields a truncated protein lacking 16 amino acids encoded by exon 7, and results in reduced biochemical stability due to a degradation signal known as Degron (Lorson et al., 1999; Monani et al., 1999; Cho et al., 2010). The differences between *SMN1* and *SMN2* are summarized in **Figure 3**. The chromosomal region that contains the *SMN* gene is highly unstable and conversion events of *SMN1* to *SMN2* are common and consequently result in various *SMN2* copy numbers (Sumner, 2006). While all forms of SMA are caused by deletions or mutations in *SMN1*, the copy number of *SMN2* could modulate the severity of the disease. This is due to the fact that 10% of the expressed *SMN2* is the full length protein and consequently genotype/phenotype analysis reveals that clinical severity is inversely proportional to *SMN2* copy number making SMA a dosage sensitive disease (Lefebvre et al., 1997). In type 1 SMA, the majority of patients have only one to two copies of *SMN2,* this is insufficient to compensate for disease severity but milder forms of SMA are associated with three or four copies of *SMN2* (Feldkotter et al., 2002).

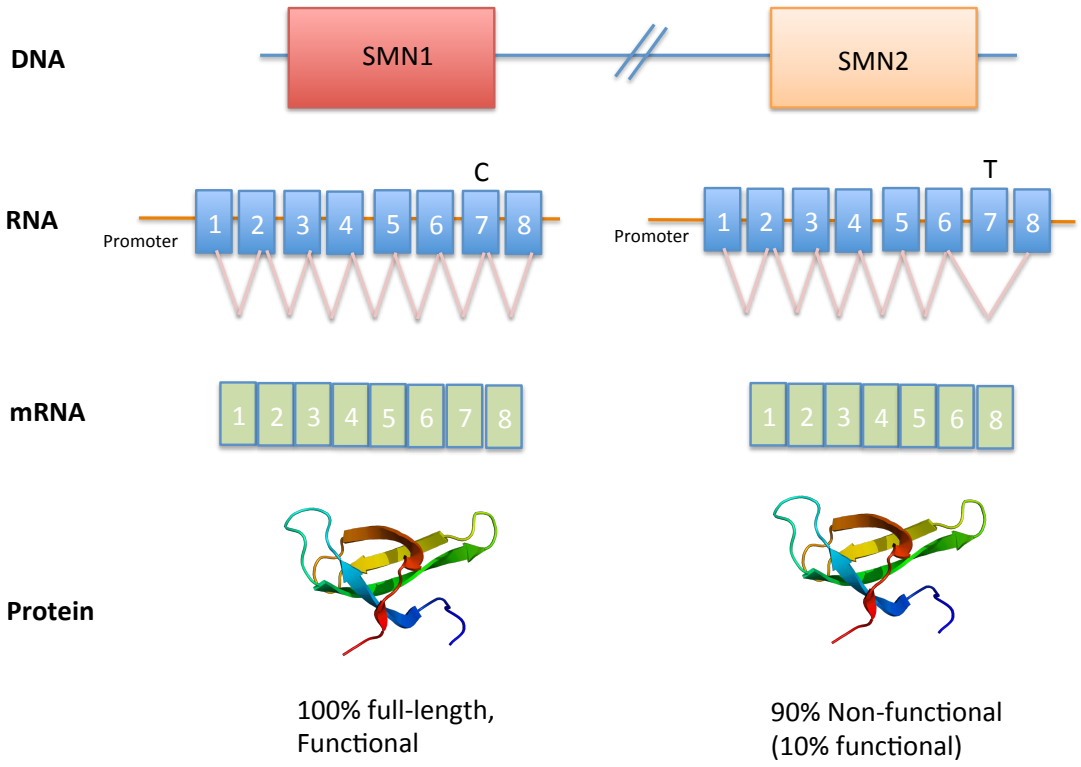

Figure 3. The difference between *SMN1* and *SMN2*

The major difference between *SMN1* and *SMN2* is a C to T transition in exon 7, this results in splicing defects and exon 7 skipping that consequently results in a non-functional protein (90%) as the major product of *SMN2*. 10% of the transcript from *SMN2* contains exon 7 and is fully functional and depending on its copy number can reduce the severity of the disease.

Function of SMN Protein

The full length SMN protein (38 kDa) is present in all cells of the developing embryo however tissue specific modulation in expression levels and developmental stage variations in expression pattern have been described (Liu et al., 2010). The SMN protein is highly conserved through evolution and all eukaryotic organisms studied to date require the protein for housekeeping functions. Knocking out the endogenous murine *Smn* leads to pre-implantation lethality (Schrank et al., 1997). The SMN protein localizes in the nucleus as well as the cytoplasm (Dreyfuss et al., 1996) and has a key function in assembling the spliceosome and global gene expression through snRNP biogenesis (Fischer et al., 1997). snRNPs are the structural units of the splicing machinery and associated problems with initiating this complex can lead to general splicing defects. It is important to note that snRNP complexes are not equally affected with reduced SMN (Lotti et al., 2012). This is an important finding and provides insight into why motor neurons are particularly vulnerable to reduction in SMN. The SMN protein is also an essential component of RNP complexes that are actively transported in neuronal processes and could in part explain the differential vulnerability of motor neurons in SMA (Zhang et al., 2003).

Multiple Organ Pathology

While mostly thought of as a motor neuron disease, recent evidence highlights the involvement of skeletal muscle in the pathophysiology of SMA (Boyer et al., 2013; Mutsaers et al., 2011; Cifuentes-Diaz et al., 2001). C2C12 myoblasts with reduced SMN expression display several defects such as abnormal proliferation, aberrant myoblast fusion, and malformed myotubes (Shafey et al., 2005). Significant disruption to the molecular composition of skeletal muscle as well as increased activity of cell death pathways in SMA muscle in pre-symptomatic severe SMA mice has been reported (Mutsaers et al., 2011). It is important to highlight that this muscle pathology was present in the absence of any detectable degenerative changes in lower motor neurons. There have been several other organs that have been implicated in the pathophysiology of SMA. Pancreatic and metabolic defects in humans and *Smn*$^{2B/-}$ mice have been reported, and *Smn*$^{2B/-}$ mice presented with fasting hyperglycemia, glucose intolerance, hypersensitivity to insulin, and hyperglucagonemia (Bowerman et al., 2012). Mutations in the murine exon 7 in the liver lead to liver failure and death and this highlights the importance of SMN in hepatic homeostasis (Vitte et al., 2004). Lung structural defects are reported in the severe Taiwanese SMA mice, which presented with discolorations of the lungs compatible with pulmonary infarctions and emphysema (Schreml et al., 2012). Intestinal problems reported in SMA mice range from impacted bowel, pneumoperitoneum, reduced numbers of villi, intracytoplasmic vacuoles, severe intramural edema in the lamina propria, and diarrhea (Le et al., 2011; Schreml et al., 2012). Cardiac abnormalities and structural defects include inter-ventricular septum (IVS) remodeling, under-

developed left ventricular wall, and dilated ventricles which in *SMN*Δ7 model precede motor neuron degeneration (Shababi et al., 2010). Therefore there are multiple organ pathologies evident in various mouse models and human case reports, and SMA can lead to multiple organ dysfunction.

Mouse Models

To better understand the pathogenesis of SMA, several mouse models of the disease have been generated. Mice only carry one copy of the *Smn* gene and knocking out the single murine *Smn* gene leads to embryonic lethality, while heterozygous ($Smn^{+/-}$) mice can be used as a model of very mild SMA (Schrank et al., 1997). Mice that lack the endogenous *Smn* gene but have 2 copies of the human *SMN2* transgene ($Smn^{-/-}$, $SMN2^{+/+}$) develop a severe phenotype (Monani et al., 2000). With an additional transgene expressing high levels of *SMN* transcript lacking exon 7 on a $Smn^{-/-}$, $SMN2^{+/+}$ background, type 1 SMA can be modeled. This model is also known as *SMN*Δ7 and has a median survival of 2 weeks (Le et al., 2005). This was an interesting observation because it implies that the exon 7-skipped protein product, *SMN*Δ7, retains a small degree of functionality and confers some phenotypic improvement. The $Smn^{2B/-}$ mice were established in our laboratory by modifying the exon splicing enhancer for exon 7. This was achieved through the 2B mutation which consists of substitution of three nucleotides in the critical AG-rich exon splicing enhancer (Bowerman et al., 2012; Hammond et al., 2010). The consequence of this substitution is alternative splicing and the predominant

production of a transcript lacking exon 7 which causes a significant reduction in the levels of full length Smn protein (DiDonato et al., 2001). The *Smn*$^{2B/-}$ mice have a phenotype that manifest shortly after 2 weeks of age and display the neurological phenotype typical of SMA. This model does not contain the human *SMN2* transgene and allows for experiments that can provide insight into the differential regulation of *SMN1* and *SMN2* under various experimental conditions.

Therapeutic Strategies

While there is no curative treatment for SMA, cell therapy, gene therapy, and small molecule therapeutic strategies aim to ameliorate the disease severity and onset. This can be achieved by introducing *Smn* via gene therapy (Foust et al., 2010; Passini et al., 2010; Azzouz et al., 2004) or to restore a defective and dysfunctional pathway downstream or independent of the *Smn* gene (Bowerman et al., 2010). In the latter example, depletion of Smn leads to increase in active RhoA which regulates actin cytoskeleton dynamics. Small molecule therapy with Y-27632 and fasudil that inhibits a downstream effector of RhoA known as Rho-kinase (ROCK), improved maturation of NMJs, increased muscle fiber size and significantly prolonged survival, and increased the

Problems in SMA	Therapeutic Target	Approach for therapy
SMN1 gene mutation	Replacement of SMN1	Gene replacement therapy
Alternative splicing of SMN2 RNA	Exon 7 inclusion	Antisense oligonucleotides **HDAC inhibitors (TSA)** Tetracycline
Decreased full length SMN2 transcript	Increased amounts of SMN transcript output	**HDAC inhibitors (TSA)** Prolactin Quinazolones
SMN protein deficiency	Stabilization of SMN protein	Proteosome inhibitors Indoprofen polyphenols
Motor neuron loss	Neuroprotection Neuromaintanance	Cell therapy Neurotrophic support **HDAC inhibitors (TSA)**

Table 2. Summary of the major therapeutic strategies used in SMA

The major therapeutic approaches in SMA in various animal and cellular models as well as human clinical trials. HDAC inhibition targets several problems in SMA pathogenesis and is a promising avenue in treating SMA.

number of motor neurons in the lumbar spinal cord (Bowerman et al., 2010; Bowerman et al., 2012). Another small molecule therapy option involves transcriptional activation of the endogenous *SMN2* gene using histone deacetylase inhibitors. This approach has been shown to modestly increase Smn protein levels (Hahnen et al., 2006; Avila et al., 2007; Rak et al., 2009). Summary of the major therapeutic strategies can be found in Table 2.

Chromatin Remodeling and Histone Acetylation

Epigenetic regulation is an essential component of proper nervous system development and function. DNA methylation is essential for the regulation of gene expression in the nervous system. Another critical type of epigenetic regulation is modification of histone proteins. Post-translational modification and specifically acetylation of histones can orchestrate the controlled expression and silencing of various genes. Under homeostatic conditions and normal cellular function, the activity of two key enzymes. Histone acetyl transferases (HATs) and histone deacetylases (HDACs) harmoniously regulate the net acetylation state and balance in their activity ensures proper cellular function. Furthermore, the interplay between these two enzymes is important in the nervous system and crucial for neuronal and glial survival (Rouaux et al., 2003; Boutillier et al., 2003). Increasing the acetylation state either through HAT overactivity or inhibition of HDAC activity through pharmacological manipulation, causes chromatin remodeling and a loosely packed organization that enhances gene transcription, while a decrease in net acetylation leads to chromatin condensation and

prevents the transcriptional machinery to access the promoter regions and leads to transcriptional repression. Class I HDACs include HDACs 1, 2, 3 and 8, and all are Zn^{2+}-dependent deacetylases and have a particular importance in various nervous system pathologies. Class IIa HDACs include HDACs 4, 5, 7, and 9, and these are also Zn^{2+}-dependent deacetylases. Class IIb HDACs include HDAC 6 and 10. HDAC 6 has a very important cytoplasmic function and deacetylates α-tubulin (Hubbert et al., 2002). Class III HDACs are known as sirtuins, which require NAD^{+} to be enzymatically functional (Blander et al., 2004). Class IV HDACs consist of a single member, HDAC 11, which resembles class I and II HDAC activity.

Histone Acetylation in Neurodegeneration

Cellular acetylation state is an extremely important and highly dynamic and regulated cellular process. The disruption of acetylation homeostasis is commonly observed in various neuropathologies involving significant cell death and loss of function (Hahnen et al., 2008; Saha et al., 2006). Furthermore, global reduction in histone acetyl transferase (HAT) activity and the consequent shifting towards over-deacetylation is commonly associated with neurodegenerative states (Rouaux et al., 2003). Therefore, the activity of HDACs seems to be stable and not prone to much change, and HAT activity changes seem to correlate with the onset of neurodegeneration and neuropathology. Transcriptional dysfunction and HAT misregulation have been associated with Huntington's disease (Steffan et al., 2000). HDAC inhibitors suppress the silencing

effects of histone deacetylases and by remodeling the chromatin structure, shift the balance towards transcriptional initiation and lead to controlled upregulation of the target genes. The therapeutic potential of HDAC inhibitors can be extended to various cancers, hematological disorders, cardiovascular diseases, and infectious diseases (Granger et al., 2008; Monneret et al., 2007; Finazzi et al., 2013). HDAC inhibitors have also been evaluated in disease models of a variety of neurodegenerative conditions such as Huntington disease, ALS and multiple sclerosis (Gardian et al., 2005; Ryu et al., 2005; Faraco et al., 2011; Hockly et al., 2003). HDAC inhibitors have been beneficial and widely used in animal models of other neurodegenerative conditions such as Alzheimer disease (Kilgore et al., 2010). The mechanism of action of HDAC inhibition is a combination of neuroprotection combined with neurotrophicity and anti-inflammation and is summarized in **Figure 4**. It should be emphasized that the exact combination of neuroprotective pathways activated through HDAC inhibition significantly differs from disease to disease and even in various models of the same disease.

HDAC inhibitors in SMA

The efficacy of HDAC inhibitors has been investigated in various cellular, animal, and human clinical trials. Sodium butyrate is a short-chain fatty acid with low toxicity, capable of increasing SMN protein levels in the lymphoid cell lines obtained from Type I, Type II and Type III patients by modifying the alternative splicing pattern of exon 7 in the SMN2 gene under the regulation of SR proteins; furthermore sodium

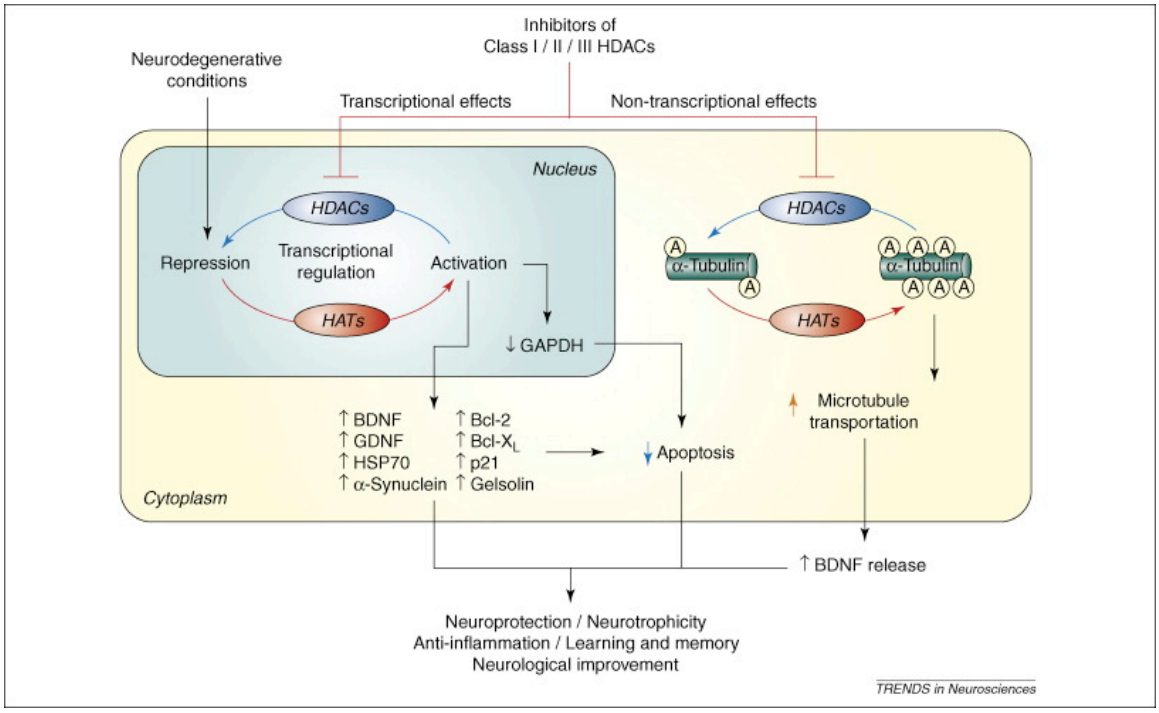

Figure 4. HDAC inhibition in neurons and neurodegenerative conditions

HDAC inhibition is protective in neurons and glial cells by taking advantage of multiple pathways. There is increase in neurotrophic support, decrease in apoptosis, improvement in cellular trafficking, and increase in the activity of various neuroprotective pathways (Chuang et al., 2009).

butyrate was able to increase Smn protein levels and improve the SMA phenotype *in vivo* using SMA-like mouse models, however the side effects and short half life limit its clinical use (Chang et al., 2001). Valproic acid (VPA) is a food and drug administration (FDA) approved drug with a terminal half-life of 8–10 h in human serum and increases SMN protein levels in the fibroblast cells obtained from type I to type III patients as well as hippocampal brain slices from rats; importantly this increase in SMN was through both AP1 and/or Sp1-dependent transcription and inclusion of exon 7 into *SMN2* mRNA via the splicing factor Htra2-b1 (Brichta et al., 2003). In another study, 1 mM VPA in SMA derived fibroblast from Japanese SMA patients increased *SMN2* expression at both the transcript and protein level through the increase in trans-acting splicing factor SF2/ASF and a decrease in the expression of heterogeneous nuclear ribonucleoprotein A1 (hnRNPA1) (Harahap et al., 2011). Furthermore VPA promoted neurite outgrowth in PC12 cells (Van Bergeijk et al., 2006) and significantly increased SMN protein levels in the lymphocytes of five out of six SMA patients (Piepers et al., 2010). Another HDAC inhibitor, suberoylanilide hydroxamic acid (SAHA) has good oral bioavailability as well as an excellent safety profile and increases Smn levels at low micromolar concentrations in several neuroectodermal tissues such as rat hippocampal brain slices and motor neuron-rich cell fractions, as well as human brain slice culture assays and has shown beneficial effects in two mouse models of SMA (Hahnen et al., 2006; Riessland et al., 2010). 4-phenylbutyrate is another HDAC inhibitor that increases *SMN2* transcript levels from 50-400% in fibroblast cell cultures from 16 SMA patients affected by different

clinical severities; interestingly milder forms of SMA responded better to PBA and had higher *SMN2* expression (Andreassi et al., 2004). Trichostatin A has shown beneficial effects in the *SMN*Δ7 mouse model that carries the human *SMN2* transgene and the beneficial effects could be synergistically extended using nutritional support (Avila et al., 2007; Narver et al., 2008). It is important to stress that the above studies demonstrate an increase in the human *SMN2* gene and there is little evidence that *SMN1* or the murine *Smn* gene responds to HDAC inhibitors. The preclinical testing phase using HDAC inhibitors in treating SMA was promising and several HDAC inhibitors were already FDA approved and in clinical use for decades to treat neurological conditions and had impressive safety profiles. This was the impetus for the start of several large scale randomized, double-blind, placebo-controlled clinical trials in humans which ended up showing no significant beneficial change in outcome measures in adults and children with various forms of SMA (Kissel et al., 2011, 2013; Swoboda et al., 2010; Mercuri et al., 2007).

Trichostatin A in treating spinal muscular atrophy

Originally isolated as an antifungal medication, the highly potent Trichostatin A (TSA) belongs to the hydroxamic acid family of HDAC inhibitors. The mechanism of action for TSA is summarized in **Figure 5**. Trichostatin A is a pan HDAC inhibitor similar to SAHA and can inhibit class I and class II HDACs (summarized in **Figure 6**). Trichostatin A requires regular administration due to its rapid absorption and metabolism.

Following intraperitoneal administration, Trichostatin A was able to reach the plasma within 2 minutes (Sanderson et al., 2004). Following plasma absorption, TSA has a relatively short half-life of 6-9 minutes and then gets rapidly metabolized to secondary byproducts, some of which display histone deacetylase activity (Sanderson et al., 2004). Another important feature of this potent HDAC inhibitor is the ability to cross the blood brain barrier and reach the brain and spinal cord (Avila et al., 2007). In the context of SMA, TSA activates the *SMN2* promoter in an *SMN2*-BLA reporter Assay (Jarecki et al., 2005). Daily intraperitoneal TSA injection from P5-P13 slightly increased Smn protein levels in the brain, spinal cord and muscle tissue of the SMNΔ7 mouse model after disease onset and was correlated with a modest improvement in survival, attenuation of weight loss, and enhancement of motor behavior (Avila et al., 2007). However, whether this beneficial effect was actually through the modest increase in Smn, or through another pathway was not clearly demonstrated. HDAC inhibition using TSA can affect the activity of many genes and it is not yet known which neuroprotective pathways are targeted by TSA in SMA. It is also important to emphasize that TSA has been shown to slightly increase Smn protein levels in models that carry the human *SMN2* transgene.

The beneficial role of TSA has been investigated in our laboratory by taking advantage of the $Smn^{2B/-}$ intermediate mouse model of SMA. The $Smn^{2B/-}$ mouse does not contain the human *SMN2* transgene and instead harbors a three nucleotide substitution in exon 7 of the endogenous *Smn* gene and consequently displays an intermediate phenotype

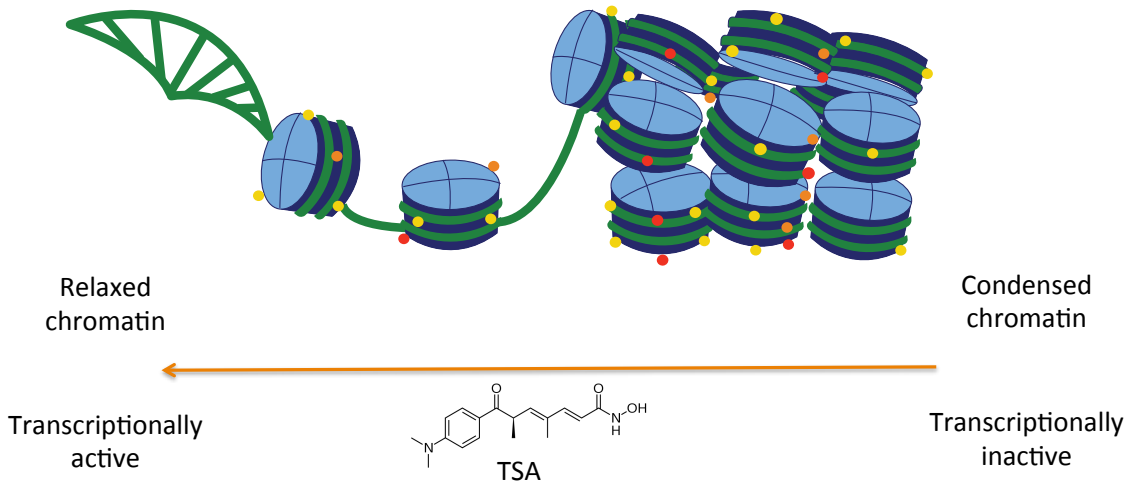

Figure 5. Schematic demonstrating the mechanism of action of TSA

TSA acts as an HDAC inhibitor and can activate the transcriptional machinery and enhance the production of many genes by relaxing the chromatin architecture.

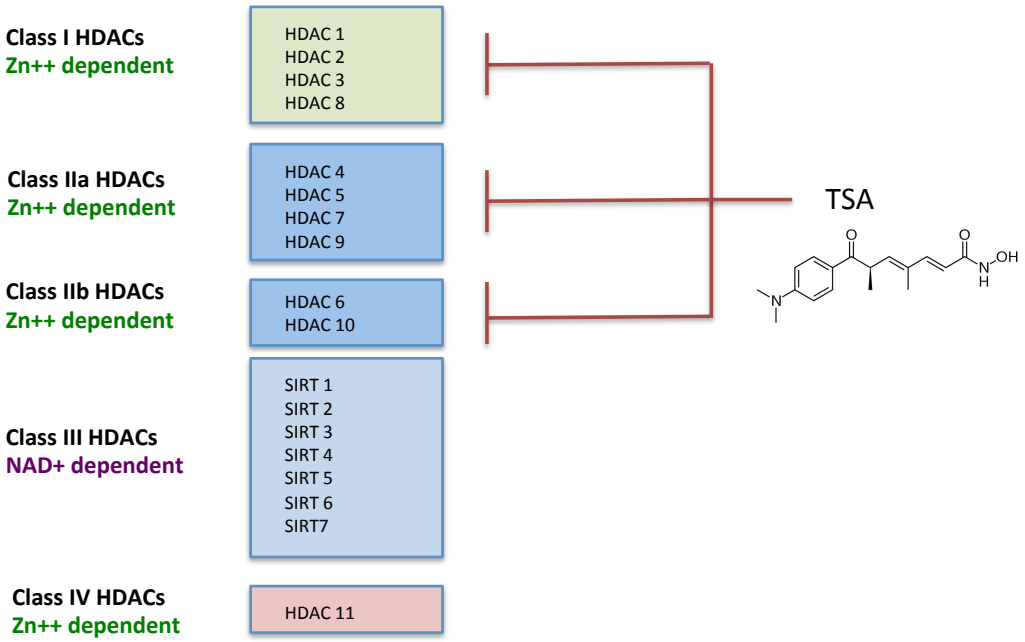

Figure 6. Schematic demonstrating the HDAC inhibition potential of TSA

TSA is able to non-specifically inhibit the zinc-dependent class I and class II HDACs with high potency (Adapted from Chuang et al., 2009).

(Hammond et al., 2010; Bowerman et al., 2012). The features of SMA are present as early early as the second week of life in the *Smn*$^{2B/-}$ mice when compared to *Smn*$^{2B/+}$ littermate controls (Bowerman et al., 2009). To investigate the beneficial effects of TSA, *Smn*$^{2B/-}$ mice were administered TSA or vehicle (DMSO) daily from postnatal day (P) 12 to 25. Preliminary findings from our laboratory showed that TSA treatment significantly improved survival, reduced weight loss, and improved motor behavior in *Smn*$^{2B/-}$ mice (Unpublished data, Dr. Hong Liu). TSA was able to reduce motor neuron loss in the spinal cord of *Smn*$^{2B/-}$ mice (Unpublished data, Dr. Hong Liu). The phenotypic improvements conferred by serial TSA treatment are summarized in **Figure 10**. The beneficial mechanism to explain the improvements in phenotype and the reduction in motor neuron death is unclear. It is of particular interest to know whether the beneficial effects are through an increase in Smn protein levels. Previous studies using TSA in mouse models of SMA have attributed the improvements in phenotype to a modest increase in Smn protein levels (Avila et al., 2007). However it is important to note that many genes that respond to TSA are involved in neuromaintenance and neuroprotection, and the orchestrated activity of these genes may contribute to the improvement in phenotype that is observed. HDAC inhibitors have also been used in a variety of other neurodegenerative conditions and have yielded positive outcomes. The beneficial effects in various other neurodegenerative conditions have been attributed to multiple neuroprotective pathways and it is likely that TSA takes advantage of multiple neuroprotective targets to confer protection in SMA.

Hypothesis and Objectives

We hypothesize that the beneficial effects of TSA on the SMA phenotype act primarily through Smn-independent pathways. The objectives of this thesis are to investigate the effects of TSA on Smn levels from various cells and tissues obtained from *Smn*$^{2B/-}$ mice. We have the following specific aims:

1) Investigate the effects of TSA on Smn protein and transcript levels in various tissues and cells obtained from *Smn*$^{2B/-}$ mice.

2) Assess the effects of TSA on specific pathways known to be perturbed after Smn depletion in the *Smn*$^{2B/-}$ mice.

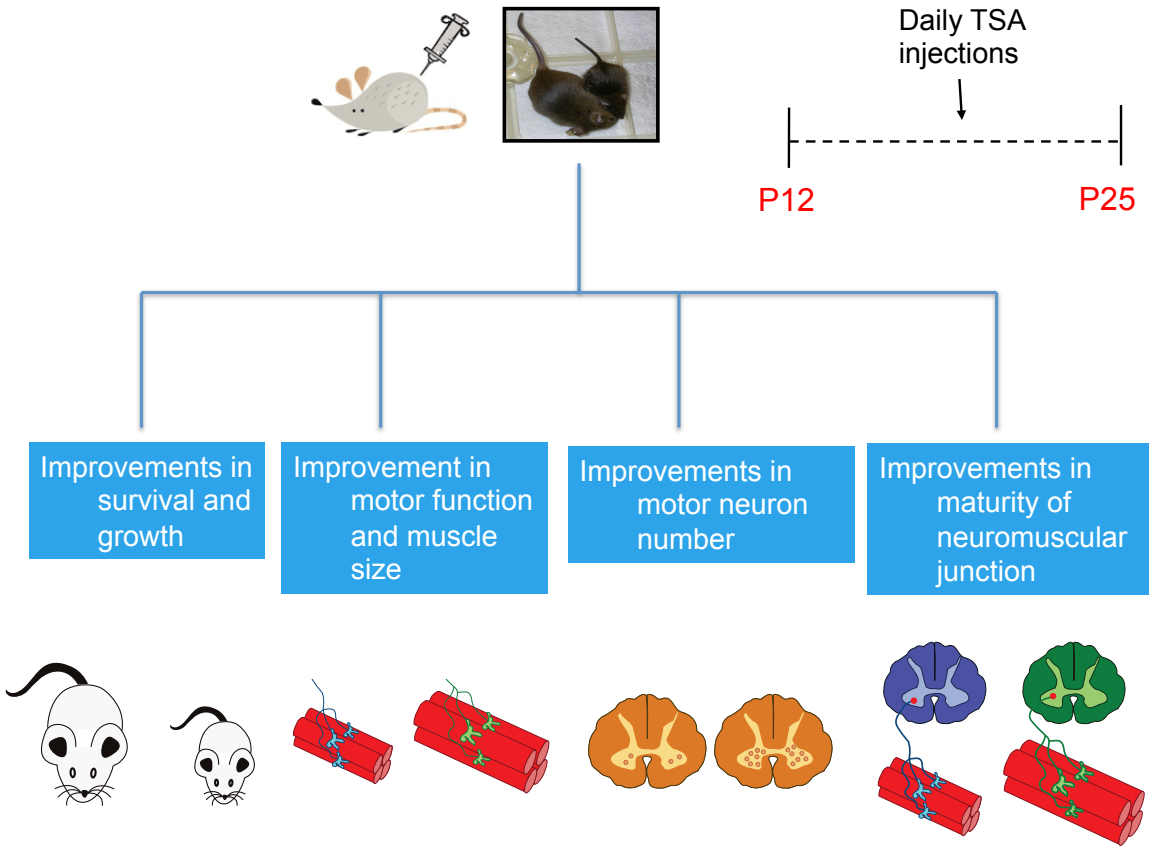

Figure 7. Schematic summarizing the beneficial effects of TSA in *Smn*$^{2B/-}$ mice.

Serial TSA treatment from P12-P25 in the *Smn*$^{2B/-}$ mice leads to significant improvements in survival and growth. Histological examination reveals improvements in myofiber size, neuromuscular junction maturity, and motor neuron number in the spinal cord. The mechanism for these beneficial effects is however unclear.

Materials and Methods

Animals

The intermediate SMA mouse model, $Smn^{2B/-}$, was established in our laboratory and maintained on a C57BL/6 x CD1 hybrid background (Bowerman et al., 2012; Hammond et al., 2010). The 2B mutation consists of a substitution of 3 nucleotides in the exon splicing enhancer of exon 7 that consequently reduces the production of full length Smn protein (DiDonato et al., 2001). The $Smn^{+/-}$ mice were obtained from Jackson Labs and were crossed with $Smn^{2B/2B}$ mice to produce $Smn^{2B/-}$ affected mice and $Smn^{2B/+}$ control littermates. The $Smn^{2B/+}$ littermates did not display any detectable phenotype and were used as controls. Wild type mice were used as a secondary control for biochemical analysis. The wild type (WT) mice are also on a C57BL/6 x CD1 hybrid background.

TSA Administration, intra-peritoneal injection

Mice were weighed daily and received intra-peritoneal (IP) injections of DMSO or TSA. TSA was dissolved in DMSO at a concentration of 4 μg/μL. Mice were administered TSA at a dosage of 10 mg/kg of body weight or vehicle DMSO daily from postnatal day (P)12 to P25 using a 33-gauge needle. The requirement for daily injection of TSA is due to its rapid pharmacokinetics and a plasma half-life of approximately 5-10 minutes following rapid plasma absorption of approximately 2 minutes (Sanderson et al., 2004). Soft bedding, water-soaked food cubes and transgel were provided to the young pups in TSA- and vehicle-treated groups after weaning age of P21. Warm pads were also provided under the cages from P21 to P25. The University of Ottawa Animal Care

Committee approved all experimental protocols. The protocols conformed to or exceeded those defined in the Canadian Council on Animal Care's Guide to the Care and Use of Experimental Animals, and the Animals for Research Act. Endpoints were as per veterinary recommendation (severe dehydration, low body temperature and deserted by feeding mother). Genotyping was performed by PCR using genomic DNA extracted from tails of mice.

SDS-PAGE and western blot analysis

To harvest tissues for protein analysis, mice were sacrificed by cervical dislocation two hours after the last TSA injection. Brains, spinal cords, heart, hind limb muscle and livers were dissected using sterile techniques. Post extraction, the tissue was frozen in liquid nitrogen and stored at -80ºC. Protein extracts were prepared, and sodium dodecyl sulfate Polyacrylamide gel electrophoresis (SDS-PAGE) and western blot performed. The brain, spinal cord, hind limb muscle, liver, and heart obtained from the *Smn*$^{2B/-}$ mice post TSA or DMSO injection was homogenized in lysis buffer (50 mM Tris-HCl, pH 7.4, 150 mM NaCl, 1 mM EDTA, 1% NP-40, and 1% glycerol) supplemented with 1 mM PMSF, 0.01 mg/ml leupeptin, 0.01 mg/ml aprotinin, 1 µl/ml pepstatin, and 100 µM Na3VO4 (Sigma). The protein lysate was stored at -80ºC until further use. Protein concentration was determined by Bradford assay with Bio-Rad dye following the manufacturer's instructions. Protein gel electrophoresis and western blot were performed according to standard protocols. Following this step, we performed incubation with the various antibodies (see western blot antibodies section). Pierce ECL detection kit (Thermo Scientific Pierce ECL Western Blotting Substrate) was used to detect the protein products. All the quantification analysis and densitometric analyses were performed

using ImageJ software (NIH) and Microsoft Excel. Immunoblot data are expressed as ratios using actin, GAPDH or tubulin (for the differentiated myotube data) as a loading control for normalization.

Histone isolation and western blot analysis

Histone isolation was performed using the protocol adapted from Mishra et al. (Mishra et al., 2003). One hundred mg of brain or liver tissue was homogenized using PowerGen tissue homogenizer (Fisher Scientific) in 500 µl of ice cold histone lysis buffer (10 mM Tris-HCl, pH 6.5, 50 mM sodium bisulfite, 1% Triton X-100, 10 mM $MgCl_2$, and 8.6% sucrose). For nuclear fraction isolation, the samples were centrifuged at low speed (1000 g) for 10 minutes. This was followed by two additional washes in cold lysis buffer and once with cold Tris-EDTA (10 mM Tris-HCl, pH 7.4, and 13 mM EDTA). The nuclei were then resuspended in 100 µl of cold water followed by acidification with hydrochloric acid at a final concentration of 0.2 M. The samples were vortexed and placed on a rotator for 1 hour. Acid soluble proteins were obtained using centrifugation at 15,000 *g* for 10 minutes and were precipitated in 1 ml acetone overnight at 25°C. Following this step, acetone precipitated proteins were collected by centrifugation at 15,000 *g* for 10 minutes and the protein pellets were air dried and suspended in 50 µl water. The Bradford assay was used for determination of protein concentration. SDS-PAGE and western blot were performed and the membranes were probed with a rabbit anti-acetylated H3 histone antibody (Millipore; 1:5000), rabbit anti-acetylated H4 histone antibody (Millipore; 1:5000) and anti-pan H3 histone antibody (Millipore; 1:2000) visualized with a peroxidase-linked goat anti-rabbit IgG secondary antibody (Chemicon;

diluted 1:10,000) by chemiluminescence detection (Thermo Scientific Pierce ECL Western Blotting Substrate). Densitometry was performed using Image J software and acetylated histone H3 were normalized to pan-histone H3 values.

Western Blot Antibodies

The primary antibodies used were as follows: mouse monoclonal anti-Smn (BD Transduction Laboratory; 1:5000), anti-β-tubulin (Developmental Studies Hybridoma Bank of Iowa; clone E7; 1:500), mouse monoclonal anti-pan actin (Fitzgerald; 1:1000), mouse monoclonal anti-acetyl histone h3 (Millipore; 1:5000), mouse monoclonal anti-histone H3 (Millipore; 1:2000), mouse monoclonal anti-GAPDH (Abcam; 1:5000), MRF4 (Santa Cruz), MyoD (BD Transduction Laboratories), myogenin (BD Transduction Laboratories), Pax7 (BD Transduction Laboratories). The secondary antibodies used were as follows: horseradish peroxidase-conjugated goat anti-rabbit immunoglobulin G (Bio-Rad Laboratories, Hercules). Horseradish peroxidase-conjugated goat anti-mouse immunoglobulin G (Bio-Rad Laboratories, Hercules). Table 3 is a list of antibodies used in the present thesis.

Cell culture and drug treatment

Smn$^{2B/-}$ primary myoblasts were isolated from hind limb muscles of 3-week-old mice as originally described (Rando and Blau, 1994). The obtained primary myoblasts were cultured on collagen-coated plates (Gibco) and maintained under growth conditions using Hams F10 (Wisent) media supplemented with 20% fetal bovine serum, 2.5 ng/ml

Antibody	Concentration	Host	Company
Smn	1:5000	Mouse	BD Transduction Laboratory
Actin	1:1000	Mouse	Fitzgerald
Tubulin	1:5000	Mouse	Developmental Studies
Pax7	1:250	Mouse	BD Transduction Laboratories
MyoD	1:750	Mouse	BD Transduction Laboratories
MyoG	1:250	Mouse	BD Transduction Laboratories
Gapdh	1:10000	Mouse	Abcam
Acetylated Histone H3	1:5000	Rabit	Millipore
Acetylated Histone H4	1:5000	Rabit	Millipore
Total Histone H3	1:2000	Rabit	Millipore

Table 3. List of antibodies used in the present study with concentrations, hosts, and the company.

human recombinant basic fibroblast factor (Invitrogen), and 2% penicillin/streptomycin (Gibco). In all experiments, cells were maintained at 37°C with 5% CO_2 and were provided fresh media every second day. The cells were grown and treated with 100 nM of TSA or DMSO immediately added to the media prior to each use for a 24 hr period and were maintained at 37°C with 5% CO_2. For nuclear extraction, the cells were then harvested after 2 washes with PBS and trypsinized and pelleted followed by an additional wash in PBS. The cells were pelleted and resuspended (2-10×10^6 cells/ml) in hypotonic buffer (10 mM Hepes pH 7.9, 1.5 mM $MgCl_2$, 10 mM KCl, 0.5 µl 1 M DTT/mL, 1 µl 200 mM PMSF). After resuspension, the cells were placed on ice and allowed to incubate for 5 minutes. The cells were centrifuged at 13000 rpm for 15 sec at 4°C. Hypotonic buffer was added at half the volume with 0.15 % NP-40 and the cells were incubated on ice for 5 minutes. The cells were then centrifuged at 13,000 rpm for 15 sec at 4°C and the nuclei was suspended in 0.2N HCL and placed on a rotator at 4°C overnight. The cells were then centrifuged at 13,000 rpm for 15 minutes at 4°C and the supernatant that contains the histone proteins were obtained for concentration measurements. For the total protein isolation, the cells were treated with various doses of TSA (100-500 nM) for a 24 hr period and were maintained at 37°C with 5% CO_2. The cells were then washed twice with ice cold PBS and lysed using RIPA buffer. After the lysis of cells on ice for 10 minutes, the cells were then centrifuged at 13,000 rpm for 15 minutes and the supernatant was obtained for quantification.

$Smn^{2B/-}$ primary mouse embryonic fibroblasts were obtained from pregnant female mice at day 13 post coitum. The pregnant female mice were sacrificed by IP injection of 0.5 mL of 2.5% avertin and cervical dislocation. The uterine horns were dissected and

rinsed with 70% ethanol and placed in PBS. Each embryo was carefully separated from the placenta and surrounding tissue and the brain and dark red organs were dissected out. The dissected head was used for genotyping performed by PCR using genomic DNA. The embryo was then washed with fresh PBS and blood was removed from the tissue. The embryo was then finely minced using razor blades and PBS. After this step, the obtained tissue was suspended in 2 mL of ice cold trypsin-EDTA and using gentle shaking was incubated at 37°C for 15 minutes. After sedimentation, the suspension was then transferred to a 50 mL Falcon tube and mixed with 2 volumes of fresh mouse embryonic fibroblast (MEF) media which contains high glucose DMEM supplemented with 10% FBS, 1% L-glutamine, 1% pen-step. After incubation, the supernatant was removed and was subjected to low speed centrifugation for 5 minutes and the resulting pellet was resuspended in fresh warm MEF media and plated into a 10 cm dish. Each embryo was plated into a separate 10 cm dish and was maintained at 37°C with 5% CO_2 until cells reached confluency (1-2 days). The experiments were performed at the 4^{th} passage and confluent plates were treated with TSA (100-500 nM) or DMSO for a 24 hr period. After treatment, the cells were lysed and total and nuclear protein was obtained. For nuclear protein isolation, the cells were harvested after 2 washes with PBS and trypsinized and pelleted. The pellet was then washed with 10 ml of PBS and centrifuged at 300 g for 10 minutes. The pellet was then resuspended in 1 ml of hypotonic lysis buffer containing 10 mM Tris-HCl pH 8.0, 1 mM KCL, 1.5 mM $MgCl_2$ and 1 mM DTT and incubated for 30 minutes on a rotator at 4°C. The intact nuclei preparation was centrifuged at 10,000 g for 10 minutes at 4°C. The pellet was then re-suspended in 0.5 ml

of 0.2 N HCL and incubated overnight on a rotator. The samples were then centrifuged at 16,000 g for 10 minutes and the supernatant was obtained for quantification.

Reverse-transcription

To harvest tissues for mRNA analysis, mice were sacrificed by cervical dislocation two hours after the last TSA injection. Brains, spinal cords were dissected, frozen in liquid nitrogen and stored at -80ºC. Total RNA was isolated using RNeasy Mini Kit (Qiagen) according to manufacturer instructions from the brains and spinal cords of the TSA and DMSO treated $Smn^{2B/-}$ mice. After the extraction of total RNA, the concentration and quality of RNA were determined using the Nanophotometer spectrophotometer (MBI Lab Equipment). After ensuring the obtained RNA had sufficient quantity and quality, we performed a reverse transcription reaction. Genomic DNA was eliminated using 1 ul of DNaseI (gDNA wipeout buffer, Qiagen). Using the quantitect reverse transcription kit (Qiagen), the RNA was then reverse transcribed into cDNA according to manufacturer's protocol. The experiments were all performed with special care in an RNase free zone and in parallel with negative control samples composed of RNase/DNase free water. Following the reverse transcription, we stored the cDNA at 4°C until use in quantitative real-time polymerase chain reaction (qPCR) experiments.

Semi-quantitative RT-PCR analysis

Semi-quantitative PCR was performed with the following primers: *Smn* long (194-1117): Forward 5' GCA CAG CCA GAA GAA AAC CT 3', Reverse 5' CGA CAC GCA CAC TCC ACT 3'; *Follistatin*: Forward 5' CCT TTC AAG TGG ATG ATT TTC

3', Reverse 5' ACA GTA GGC ATT ATT GGT CTG 3'; *β-actin*: Forward 5' CCG TCA GGC AGC TCA TAG CTC TTC 3', Reverse 5' CTG AAC CCT AAG GCC AAC CGT 3'.

Quantitative Real-Time Polymerase Chain Reaction

For qPCR, 1 µL of cDNA was used in a total reaction volume of 20 µL Supermix (BIORAD) according to the manufacturer's instructions. The PCR reaction was performed on a CFX connect (BIORAD) qPCR system with 40 amplification cycles. Changes in gene expression after TSA treatment were quantified based on the $2^{\Delta CtDMSO-\Delta CtTSA}$ value. Ct was normalized to *Gapdh* (ΔCt=Ct target gene-Ct *Gapdh*). Triplicate samples were used for each PCR run. Primers include: *Smn* (final concentration at 50 nM): Forward 5' GCC ACA ACT CCC TTG AAA CAG 3', Reverse 5' TCG GGG AAA GTA GGT CAG ATA AG 3'; *Gapdh* (50 nM): Forward 5' TGA AGG GGT CGT TGA TGG 3', Reverse 5' AAA ATG GTG AAG GTC GGT GT 3'.

Muscle Histology

Histological analyses of the tibialis anterior (TA) muscle was performed for measuring myofiber size. The cross-sectional area of the TA muscle from $Smn^{2B/-}$ mice treated with either DMSO or TSA was calculated by tracing the contour of myofibers using the tracing tool in ImageJ. A minimum of 200 myofibers were traced. Cross-sections from control and SMA model mice were collected from the same area of the TA muscle.

Immunohistochemistry

For neuromuscular junction analysis, muscles were labeled by immunohistochemistry as described previously (Murray et al., 2008). Briefly, muscles were immediately dissected from recently sacrificed mice and fixed in 4% paraformaldehyde (Electron Microscopy Science) in PBS for 15 min. Post-synaptic acetylcholine receptors (AChRs) were labeled with alpha-bungarotoxin for 30 min. Muscles were permeabilized in 2% Triton X-100 in PBS for 30 min, then blocked in 4% bovine serum albumin/1% Triton X-100 in PBS for 30 min before incubation overnight in primary antibodies [neurofilament (NF; 2H3) - Developmental Studies Hybridoma Bank; synaptic vesicle protein 2 (SV2) - Developmental Studies Hybridoma Bank] and visualized with DyLight-conjugated secondary antibodies [DyLight goat anti-mouse; all 1:250, Jackson]. Muscles were then whole-mounted in Dako Fluorescent mounting media. Images were taken with a Zeiss LSM-510 Meta confocal microscope. For satellite cell quantification in the hind limb muscles obtained from the the $Smn^{2B/-}$mice, cross-sections (10-12 μm) were collected using a cryostat (Leica) and fixed with 4% paraformaldehyde and then stained with Pax7 antibody using a standard protocol. A mouse-on-mouse kit (Vector Labs), and the primary antibodies targeting Pax7 (Developmental Studies Hybridoma Bank, DSHB) and laminin (Abcam) were used to highlight satellite cells and the basal lamina, respectively. All secondary antibodies were purchased from Molecular Probes and nuclei were visualized using 4',6-diamidino-2-phenylindole (DAPI, Sigma). Immunofluorescence images were captured using a Zeiss Axioplan fluorescence microscope or a Zeiss Confocal microscope (LSM 510 Meta DuoScan). Pax7 positive cells were quantified from 2 different fields of view taken at

20x and expressed relative to the total number of myofibers present as assessed by laminin staining.

Statistical analysis

Statistical analyses were done with Microsoft Office Excel and GraphPad Prism software (San Diego, CA). Analysis for statistical significance between groups was performed in Microsoft Excel. The data set for each genotype and treatment group was compared to achieve the P value by Student's t-test (two-sample assuming equal variances and two-tailed). Y-axis values in the graphs were expressed as mean +/- standard deviation (SD) or standard error of the mean (SEM). $P < 0.05$ was considered to indicate statistical significance.

Results

TSA acts as an HDAC inhibitor and leads to an accumulation of acetylated histone H3 and H4 in different cells in culture

TSA treatment increases the acetylation status of histone H3 and H4 in astrocyte rich cultures

To demonstrate that TSA is active and able to function as an HDAC inhibitor, wildtype mixed glial cultures rich in astrocytes were cultured and grown until reaching a confluent stage. These cells were then treated with 100 nM of TSA or DMSO for a 24-hour period and maintained at standard culture conditions. The cells were then harvested and underwent nuclear extraction and histone purification. Western blot analysis was performed and the activity of TSA was evidenced by the increase in the acetylation status of histone H3 and H4 (**Figure 8**). The levels acetylated histone H3 and H4 were compared with total histone H3 levels. The cells were able to tolerate TSA and there was no observed toxic effects or cell death at 100 nM of TSA treament.

TSA treatment increases the acetylation status of histone H3 in $Smn^{2B/-}$ MEFs

To further show that TSA leads to an increase in acetylated histone H3 *in vitro*, we used mouse embryonic fibroblasts and treated them with 100 nM of TSA or DMSO for a 24 hour period under standard culture conditions. *$Smn^{2B/-}$* mouse embryonic fibroblasts were obtained, cultured and passaged 3 times. When the cells reached a confluent stage in

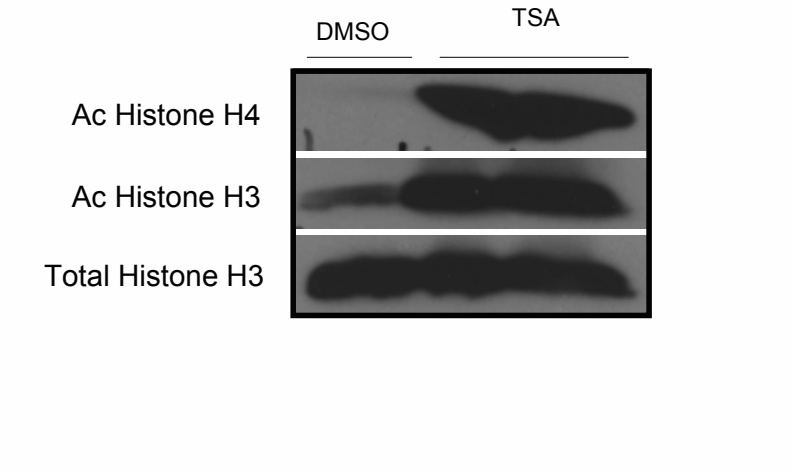

Figure 8. TSA results in an increase in the acetylation status of Histone H3 and H4. Astrocyte rich cultures obtained from wild type mice treated with 100 nM of TSA or vehicle DMSO for 24 hours and maintained at standard culture conditions. TSA treated group shows accumulation of histone H3 and H4 compared with the vehicle DMSO. Total histone H3 serves as a loading control. Lane 1 represents DMSO treated cells and Lanes 2 and 3 represent the TSA treated cells.

the third passage, they were treated with 100nM TSA or DMSO for 24 hours. Nuclear protein extraction and histone purification was performed and western blotting confirmed that TSA is able to increase acetylated histone H3 in the *Smn*$^{2B/-}$ derived mouse embryonic fibroblasts (**Figure 9A**). The cells did not show any toxicity signs and had a tolerance for 100 nM of TSA. The accumulation of acetylated histone H3 after treatment with TSA in the *Smn*$^{2B/-}$ derived MEFs confirmed that TSA is able to lead to an increase in the acetylation status of histone H3 in these cells.

TSA treatment increases acetylated histone H3 protein levels in primary myoblasts

We used another *in vitro* model to demonstrate that TSA is active and can increase acetylated histone H3. In this case, we obtained primary myoblasts from *Smn*$^{2B/-}$ mice. These muscle cells were used to demonstrate that TSA is able to increase the acetylation status of histone H3 and further validate that our preparation of TSA is active. Primary myoblasts from *Smn*$^{2B/-}$ mice were treated with 100 nM of TSA or DMSO for a 24-hour period under standard culture conditions and were then collected for protein analysis. Western blot analysis revealed that TSA is able to increase acetylated histone H3 compared with DMSO control (**Figure 9B**). TSA did not have any observable toxic effects on the myoblasts at the 100 nM dosage.

TSA is able to cross the blood brain barrier and increase acetylated histone H3 *in vivo*

TSA increases the acetylation status of histone H3 in the brains of wild type mice

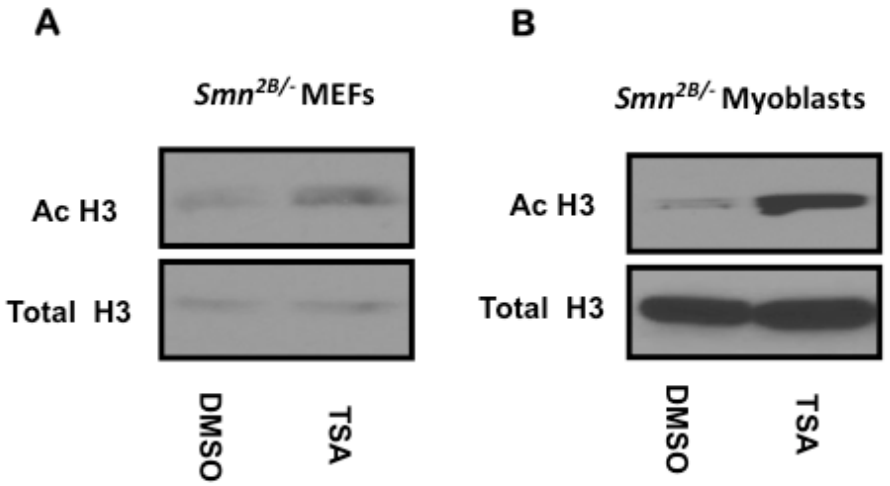

Figure 9. TSA increases acetylated histone H3 protein levels in mouse embryonic fibroblasts and primary myoblasts obtained from *Smn*$^{2B/-}$ mice.

A) Western blot analysis of primary mouse embryonic fibroblasts obtained from *Smn*$^{2B/-}$ *mice* treated with 100 nM of TSA for a 24 hour period showing an increase in acetylated histone H3 levels in the TSA treated group compared with vehicle control. **B)** Western blot analysis of primary myoblasts obtained from *Smn*$^{2B/-}$ mice treated with 100 nM of TSA for a 24 hour period showing an increase in acetylated histone H3 levels in the TSA treated group compared with vehicle control.

To assess whether TSA is able to increase the acetylation status of histone H3 in vivo, we injected wild type mice daily from P12 to P25 with TSA at a dose of 10 mg/kg. At P25, the mice were sacrificed and the brains dissected 2 hours following the final injection. Nuclear protein was extracted from the brains and western blot analysis was performed using histone H3 antibody. We determined that there is an increase in the acetylation status of H3 in the brains of wild type mice after serial injections of TSA, however this increase was not as robust as in the cell culture experiments (**Figure 10A**). This increase reached statistical significance and we can conclude that TSA is able to cross the blood brain barrier. This finding confirmed the previous studies that showed TSA can cross the blood brain barrier. This key experiment shows that under our conditions, TSA is able to reach the brain and spinal cord, both of which are important target organs in treating spinal muscular atrophy.

TSA increases the acetylation status of histone H3 in the brain of $Smn^{2B/-}$ mice

We went on to assess whether TSA is able to increase the acetylation status of histone H3 in the disease model of spinal muscular atrophy. We treated the *$Smn^{2B/-}$* mice with daily administration of TSA starting at P12 and continuing until P25. Mice received daily injections of TSA at a dose of 10 mg/kg or vehicle DMSO. On P25, the mice were sacrificed and the brain was dissected 2 hours following the last injection. Following protein extraction, nuclear histones were isolated and western blot analysis was performed using acetylated histone H3 and pan histone H3 antibodies. There was an increase in the acetylation status of histone H3 in the TSA treated SMA mice (**Figure 10B**). This increase was not as robust as the increase in acetylated histone H3 in the

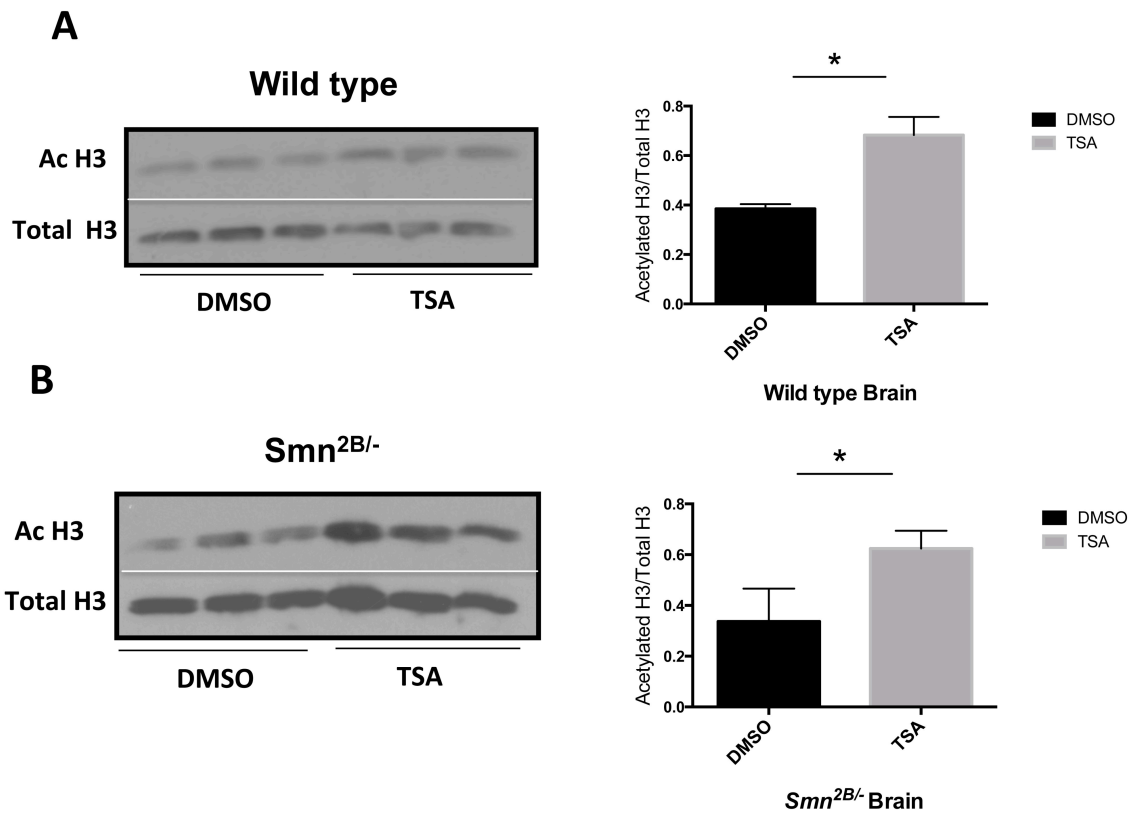

Figure 10. TSA crosses the blood brain barrier in wild type and *Smn*$^{2B/-}$ mice.

A) Western blot using brain tissue of wildtype mice treated with 10mg/kg of TSA from P12-P25 displays accumulation of acetylated histones H3 in the TSA treated group (n=3). Quantification analysis confirms the increase in acetylation levels of H3 confirming that TSA is able to cross the blood brain barrier. **B)** Western blot using brain tissue of SMA *Smn*$^{2B/-}$ mouse model treated with 10mg/kg of TSA from P12-P25 shows an increase in acetylation of histones H3 in the TSA treated group (n=3). Quantification analysis confirms the increase in acetylation levels of H3 confirming that TSA is able to cross the blood brain barrier.

Smn$^{2B/-}$ derived mouse embryonic fibroblasts or myoblasts. However, this increase did reach statistical significance and confirms that TSA is able to cross the blood brain barrier in the SMA mice. The increase in the acetylation status of histone H3 in the *Smn*$^{2B/-}$ mice was comparable to the increase in the wild type mice.

TSA does not increase Smn protein levels *in vitro*

Previous work from our lab has shown that TSA has beneficial effects in the *Smn*$^{2B/-}$ mouse model of SMA (Unpublished data, Dr. Hong Liu). Work from other laboratories on the effect of TSA on various cell and animal models of SMA concluded that the beneficial effects observed were attributable to the increase in Smn protein levels (Avila et al., 2007). We were interested in determining whether *Smn* is a direct target of TSA and investigated the effects of TSA on Smn protein levels in various cell cultures derived from wild type and *Smn*$^{2B/-}$ mice.

TSA does not increase Smn protein levels in wild type astrocyte rich cultures

Wild type mixed glial cultures rich in astrocytes were cultured and grown until reaching a confluent stage. These cultures were then treated with 100 nM of TSA or DMSO for a 24-hour period and maintained at standard culture conditions. The cells were then harvested and underwent total protein extraction. Western blot analysis was performed and the activity of TSA was confirmed through the increase in the acetylation status of histone H3 and H4. However, the TSA treated astrocyte rich cultures did not

display an increase in Smn protein levels (**Figure 11E**). Therefore TSA was unable to increase Smn protein levels in these cultures.

TSA does not increase Smn protein levels in mouse embryonic fibroblasts obtained from wild type mice

We know that TSA is able to increase acetylation status of histone H3 in wild type mouse embryonic fibroblasts. Wild type MEFs were cultured and passaged 3 times and were then treated with various doses of TSA or vehicle DMSO for a 24-hour period in standard culture conditions. Total protein was isolated after 24 hours of treatment and western blot analysis was performed to assess changes in Smn protein levels. Smn levels were not increased after 100 nM of TSA (**Figure 11A**). Therefore TSA is unable to increase Smn protein levels in wild type MEFs.

TSA does not increase Smn protein levels in mouse embryonic fibroblasts obtained from $Smn^{2B/-}$ mice

Mouse embryonic fibroblasts obtained from the $Smn^{2B/-}$ mice were cultured and passaged 3 times. We started treatment with TSA at 100 nM or DMSO for 24 hours under standard culture conditions. Treatment with 100 nM of TSA did not result in a significant increase in Smn protein levels (**Figure 11B**). To further confirm that Smn does not significantly respond to TSA, we increased the dosage to 500 nM. However, this did not increase Smn protein levels either (**Figure A1**). It should be emphasized that

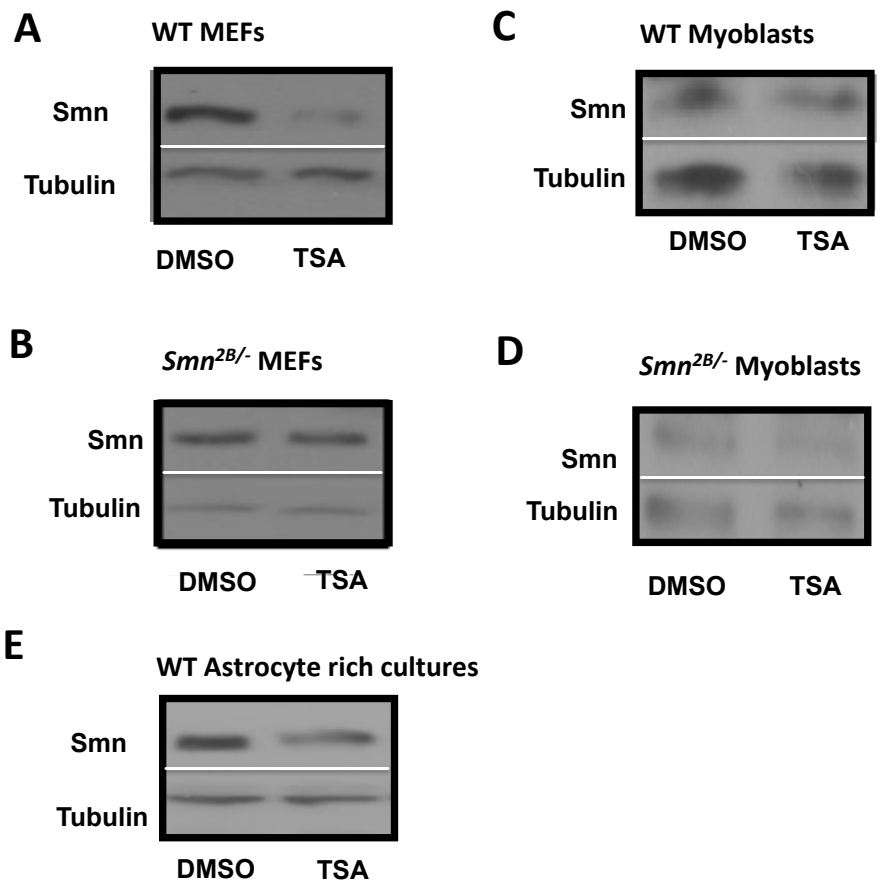

Figure 11. TSA does not increase Smn protein levels in *Smn*$^{2B/-}$ and wild type derived MEFs, Myoblasts, and astrocyte rich cultures.

A*)* Western blot showing Smn protein is not increased in the 100 nM TSA treated MEFs obtained from wild type mice. **B)** Western blot showing Smn protein is not increased in the 100 nM TSA treated MEFs obtained from *Smn*$^{2B/-}$ mice. **C)** Western blot showing Smn protein is not increased in the 100 nM TSA treated myoblasts obtained from wild type mice. **D)** Western blot showing Smn protein is not increased in the 100 nM TSA treated myoblasts obtained from *Smn*$^{2B/-}$ mice. **E)** Western blot showing Smn protein is not increased in the 100 nM TSA treated astrocyte rich cultures obtained from wild type mice.

100 nM of TSA was able to robustly increase acetylated histone H3. We therefore conclude that TSA is unable to increase Smn protein levels in *Smn*$^{2B/-}$ derived MEFs under the present conditions.

TSA does not increase Smn protein levels in primary myoblasts obtained from wild type mice

Proliferating primary myoblasts obtained from wild type mice were grown and cultured in standard culture conditions. The cells roughly reached 70% confluency prior to TSA or DMSO treatment. The cells were treated with 100 nM of TSA or vehicle DMSO for a 24-hour period. Total protein was extracted and western blot analysis was performed to assess Smn protein levels. Our analysis shows that TSA was unable to increase Smn protein levels (**Figure 11C**). This is the third cell culture model that confirmed TSA does not lead to a significant increase in Smn protein levels.

TSA does not increase Smn protein levels in primary myoblasts obtained from Smn$^{2B/-}$ *mice*

Proliferating primary myoblasts were obtained from *Smn*$^{2B/-}$ mice and grown until an approximate 70% confluent stage. The cells were then treated with 100 nM of TSA or vehicle DMSO for a 24-hour period. As before, TSA was unable to increase Smn protein levels (**Figure 11D**). Furthermore, even at a dose of 500 nM TSA, there was no increase in Smn protein levels. There were no obvious observed toxic effects at the 100 nM dose however at 500 nM, there were a small number of cells that were dying. This analysis

further increases our confidence that Smn is not a direct target of TSA in cells obtained from wild type or *Smn*$^{2B/-}$ mice. This finding is consistent with the rest of our *in vitro* data that TSA is unable to increase Smn protein levels despite being active and increasing the acetylation status of histone H3.

TSA does not increase Smn protein levels *in vivo*

TSA does not increase Smn protein levels in neuronal tissue

To determine whether the beneficial effects of TSA are due to an increase in Smn protein levels in the *Smn*$^{2B/-}$ mice, we went on to measure Smn protein levels in neuronal tissue such as brain and spinal cord. The mice were injected daily with TSA or vehicle DMSO from P12-P25 and the brain and spinal cord were dissected and underwent protein extraction. Western blot analysis was performed to quantitatively measure Smn protein levels. The results show that TSA was unable to increase Smn protein levels in the brains of *Smn*$^{2B/-}$ mice (**Figure 12A**). It should be noted that we already showed that TSA was able to cross the blood brain barrier and increase the acetylation status of histone H3. Thus, the lack of Smn induction implies that TSA does not normally target the *Smn* gene. Furthermore, serial TSA injections were also unable to increase Smn protein levels in the spinal cords of *Smn*$^{2B/-}$ mice (**Figure 12B**). There was a significant reduction in the death of motor neurons in the spinal cord (Unpublished data, Dr. Hong Liu) and this neuroprotective effect was independent of Smn protein. Therefore, other neuroprotective pathways may respond to TSA and in turn provide protection.

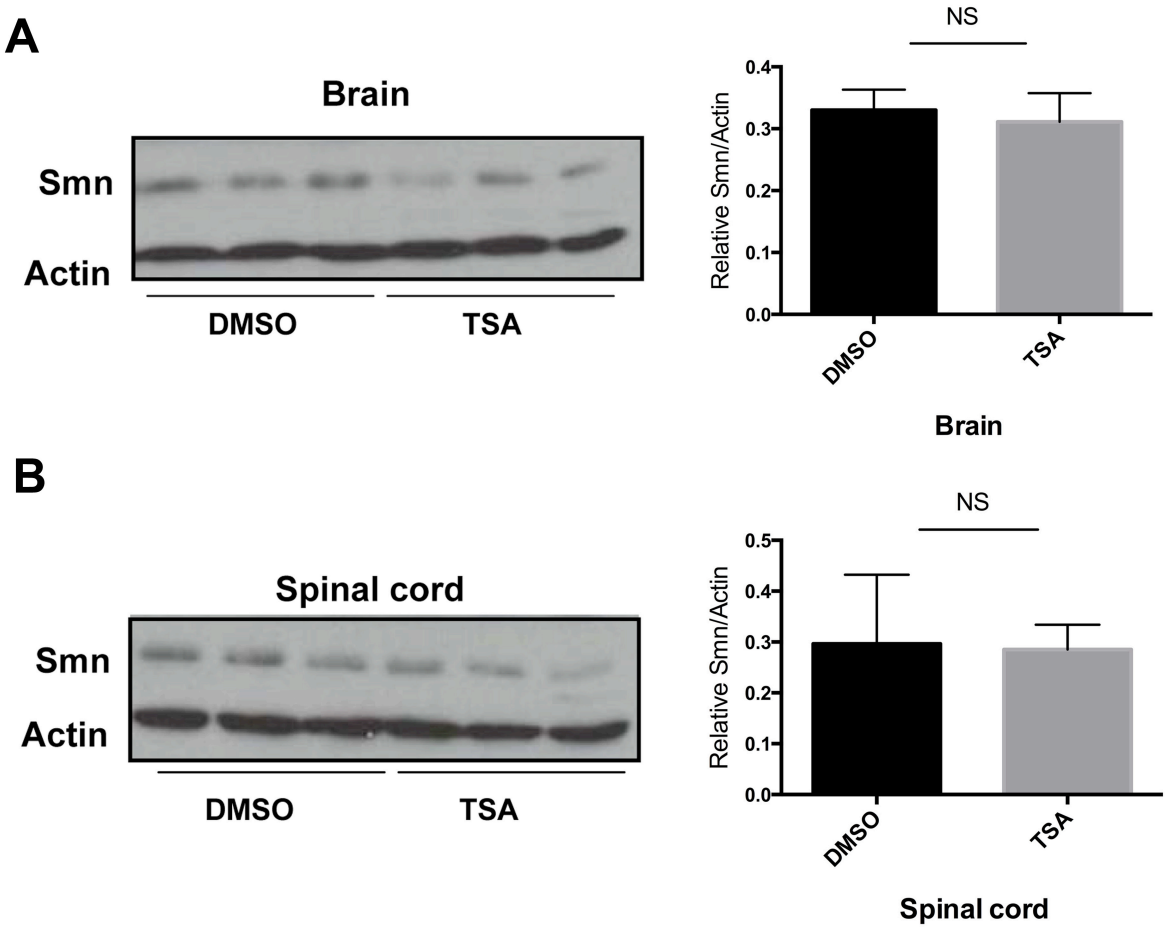

Figure 12. No changes in *Smn* protein levels in the brains and spinal cords of TSA-treated mice.

Western blot and quantification analysis revealed no significant changes in brain **(A)** or spinal cord **(B)** Smn protein levels post TSA treatment in SMA mice compared with DMSO controls (n=3).

TSA does not increase Smn protein levels in the muscle tissue

Since the Smn levels in the brain and spinal cord did not respond to TSA, we wanted to see whether TSA exerts its effects primarily by increasing muscle Smn levels. The beneficial effects in the muscle included improvements in motor behavior and growth (Unpublished data, Dr. Hong Liu) as well as increase in myofiber size. We investigated the effects of TSA in both skeletal and cardiac muscle. Serial TSA injections were unable to increase Smn protein levels in the hind limb muscle of $Smn^{2B/-}$ mice (**Figure 13A**). These results are consistent with our findings that TSA does not increase Smn protein levels in primary myoblasts obtained from $Smn^{2B/-}$ mice. TSA was also unable to increase Smn protein levels in the heart muscle obtained from $Smn^{2B/-}$ mice (**Figure 13B)**. Therefore TSA did not significantly increase Smn proteins in the muscle tissues obtained from $Smn^{2B/-}$ mice. It is important to conclude that the observed beneficial effects in the muscle such as increase in myofiber size and improvement in motor behavior is occurring independently of changes in Smn level.

TSA does not increase Smn protein levels in the Liver tissue

We investigated whether TSA leads to an increase in Smn protein levels in another non-neuronal or non-muscle tissue. TSA did not lead to a significant increase in Smn protein levels in the livers of $Smn^{2B/-}$ mice (**Figure 14**). It should be noted that recently our lab has identified metabolic defects in the $Smn^{2B/-}$ mice. Whether TSA has beneficial effects by improving these metabolic issues is unknown, however the general improvements in survival and growth after TSA administration may be due to improvements in overall metabolism.

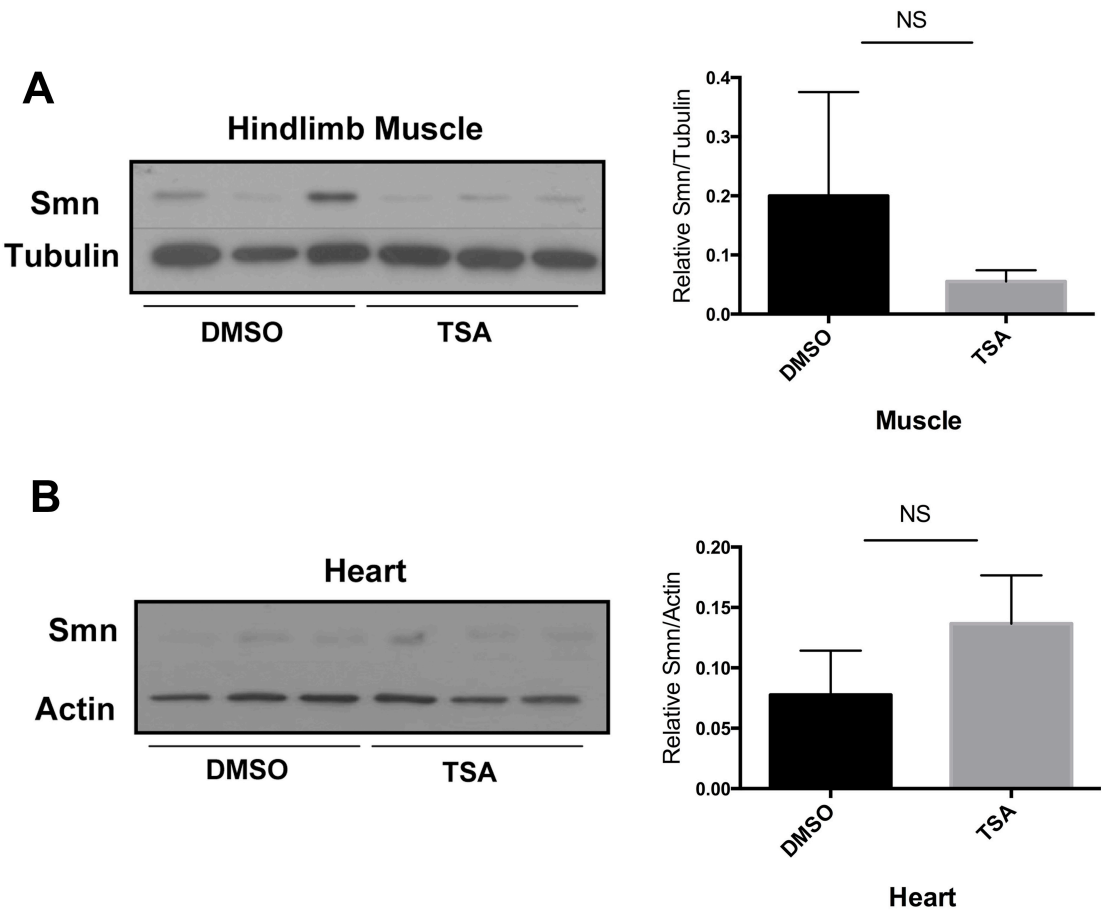

Figure 13. No changes in Smn protein levels in the hind limb muscle and heart muscle of TSA-treated mice.

Western blot and quantification analysis revealed no significant changes in hind limb muscle **(A)** or heart muscle **(B)** Smn protein levels post TSA treatment in SMA mice compared with DMSO controls (n=3).

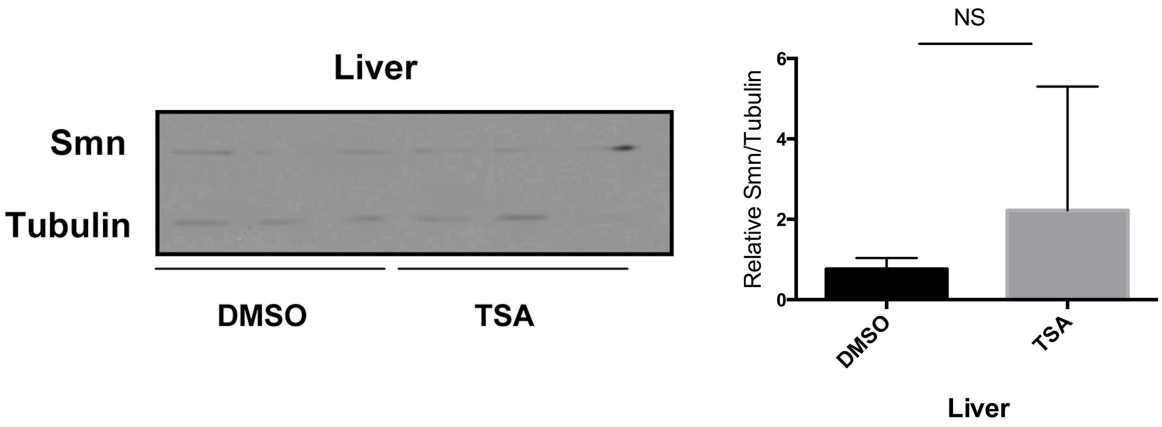

Figure 14. No changes in Smn protein levels in the liver of TSA-treated mice.

Western blot and quantification analysis revealed no significant changes in liver Smn protein levels post TSA treatment in SMA mice compared with DMSO controls (n=3).

TSA does not increase *Smn* mRNA levels in the *Smn*$^{2B/-}$ mice

TSA was unable to increase Smn protein levels in various cells and tissues obtained from the *Smn*$^{2B/-}$ mice. To further demonstrate that the murine *Smn* gene does not respond to TSA, we measured *Smn* RNA levels in the brains and spinal cords of TSA treated *Smn*$^{2B/-}$ mice. qPCR analysis revealed no significant increase in *Smn* RNA transcript levels in the brains of *Smn*$^{2B/-}$ mice after serial TSA treatment. Furthermore, TSA did not significantly increase *Smn* RNA levels in the spinal cord (**Figure 15B**); TSA does not influence splicing and there was no difference between the full length or delta 7 *Smn* RNA levels between TSA and DMSO treated *Smn*$^{2B/-}$ mice (**Figure 15A**). This experiment was conducted by Dr. Hong Liu. Therefore TSA is unable to increase total *Smn* transcript levels in the brain and spinal cord, and does not change the splicing pattern between full-length and delta 7 *Smn* transcript. Combined with our protein findings, we can conclude that *Smn* in not the major direct target of TSA in the *Smn*$^{2B/-}$ mouse model of SMA.

TSA improves the maturity of the neuromuscular junction

The effects of TSA on neuromuscular pathology was investigated by Dr. Lyndsay Murray. The *Smn*$^{2B/-}$ mouse model of SMA has widespread neuromuscular pathology. This pathology is evident by the presence of small and immature post-synaptic endplates, neurofilament accumulation, and full or partial denervation. The DMSO treated *Smn*$^{2B/-}$

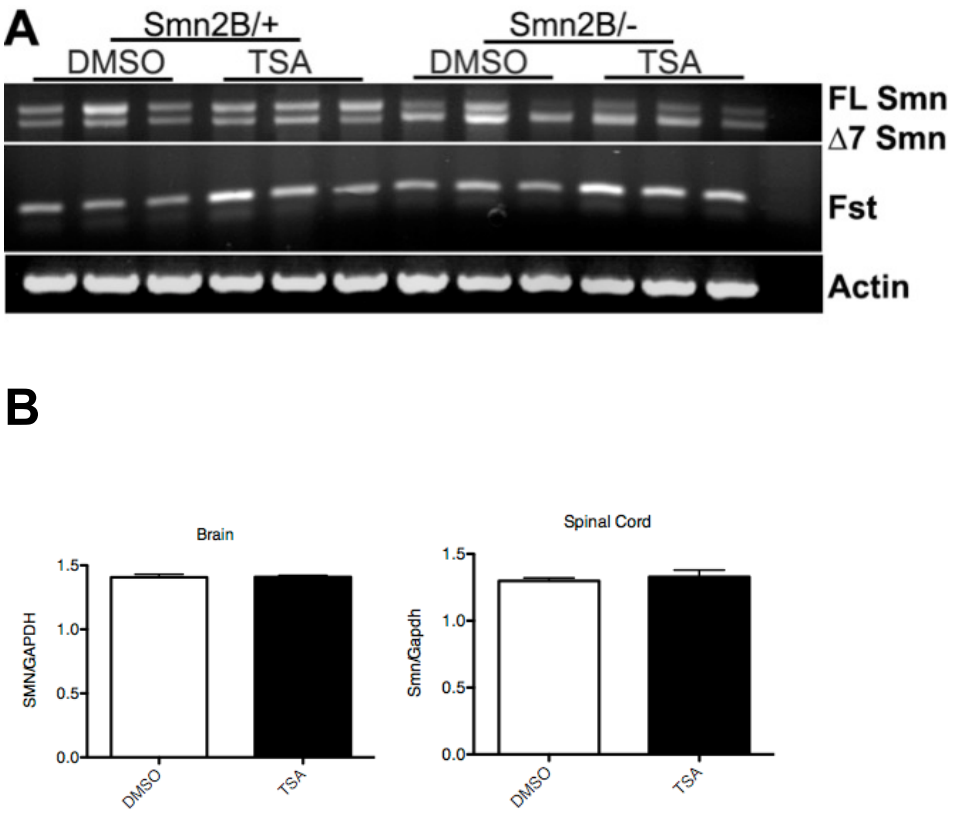

Figure 15. No alteration in the splicing pattern or levels of *Smn* mRNA in the brains or spinal cord of TSA-treated mice.

A) RT-PCR for *Smn* and a known target of TSA, *follistatin*, was conducted with total RNA extracted from brains of SMA mice or littermate controls treated with TSA or DMSO vehicle. Ratio of full length *Smn* versus *Δ7Smn* transcripts remained similar after TSA treatment in SMA or in control mice. Transcript level of *follistatin* is elevated in TSA-treated mice. *Actin* serves as a loading control. **B)** qPCR analysis revealed no significant changes in the level of *Smn* transcripts (fl+Δ7) in the brain and spinal cord of $Smn^{2B/-}$ mice after TSA treatment (n=3). Fold increase normalized to reference gene GAPDH.

mice have identical pathologies to the untreated mutant mice. TSA treated mice, however, show improvements in the maturity of the neuromuscular junctions in the transversus abdominis (TVA) as well as the rectus abdominis (RA) muscles (**Figure 16A**). There was a significant increase in the percentage of fully occupied endplates in both the transversus abdominis (TVA) and rectus abdominis muscles (RA) muscles following TSA treatment (**Figure 16B,C)**. TSA decreases the observed denervation and NF accumulation, and significantly increases post-synaptic size and maturity (**Figure 16A**). It is important to emphasize that Smn protein and mRNA transcript levels were not increased after serial TSA treatment in the brain or the spinal cord of $Smn^{2B/-}$ mice. Smn protein level was also not increased in the muscle or the primary myoblasts obtained from the $Smn^{2B/-}$ mice. Therefore, the observed improvement in neuromuscular maturity appears to be independent of Smn.

The effects of TSA on muscle

TSA increases myofiber size in the $Smn^{2B/-}$ mice

TSA has demonstrated beneficial effects in SMA muscle. The delta 7 mouse model of SMA illustrates improvement in muscle histology and function after serial TSA injection (Avila et al., 2007). We have already demonstrated that TSA is capable of improving overall growth and motor behavior in the $Smn^{2B/-}$ mice. To further investigate the mechanism underlying the improvement in motor behavior, we hypothesized that there are histological improvements in the muscle after serial TSA injection in $Smn^{2B/-}$ mice. Histological analyses were performed on hematoxylin and eosin stained cross-

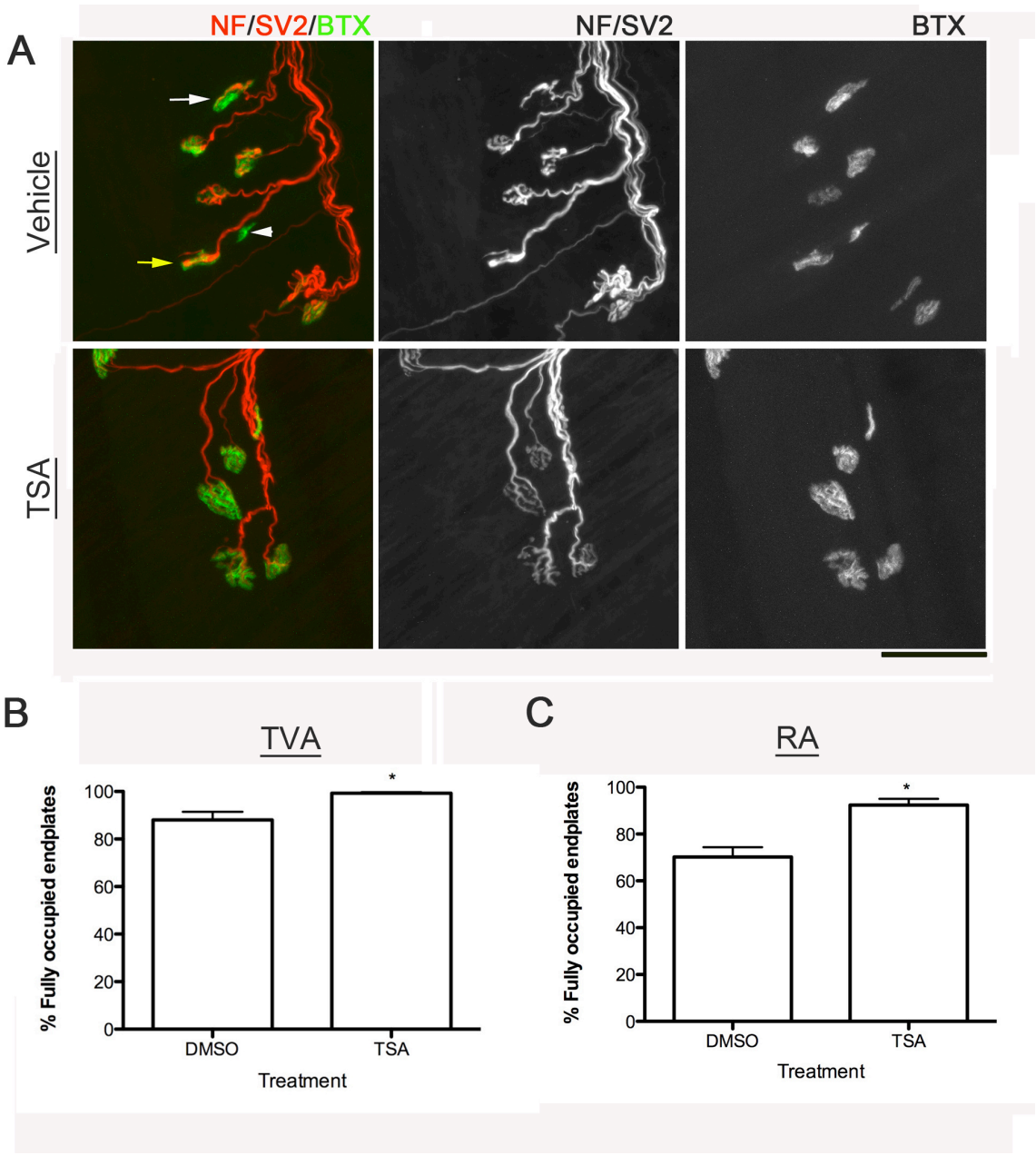

Figure 16. Maturity of neuromuscular junctions is improved in SMA mice after TSA treatment.

A) Confocal micrographs show neuromuscular junctions (NMJs) labelled with antibodies against neurofilament (NF, red) and synaptic vesicle protein 2 (SV2, red) and alpha-bungarotoxin (green). Note that whilst there is widespread NMJ pathology in vehicle treated mice, as evidenced by full/partial denervation (white arrowhead/arrow

respectively), NF accumulation (yellow arrow) and small, immature post synaptic endplates, NMJs appear much more healthy in TSA treated mice, as evidenced by a decrease in denervation and NF accumulation, and an increase in post-synaptic size and maturity. (Scale bar = 50 μm) (B, C) Bar charts show an increase in the percentage of fully occupied endplates in both the transversus abdominis (TVA; **B**) and rectus abdominis muscles (RA; **C**) muscles following TSA treatment. * $P<0.05$ by Mann Whitney test.

sections (10 μm) from frozen TA muscles of P25 *Smn*$^{2B/-}$ mice. Sections were stained with hematoxylin and eosin using a standard protocol. The decrease in myofiber size and an increase in the number of immature myofibers are two key and hallmark features of spinal muscular atrophy and are evident in the *Smn*$^{2B/-}$ mice. TSA is able to significantly increase the myofiber size in the tibialis anterior muscle of *Smn*$^{2B/-}$ mice (**Figure 17A**). Furthermore TSA is able to lead to a significantly fewer small caliber fibers and an increased proportion of large caliber fibers in muscles of *Smn*$^{2B/-}$ animals.

TSA reduces central nucleation in muscles from the Smn$^{2B/-}$ *mice*

Central nucleation corresponds to immature muscle fibers and is a key hallmark of many neuromuscular disorders (Greenfield et al., 1957; Mckeran et al., 1979). Central nucleation is observed at the pre-phenotype and phenotype stage in *Smn*$^{2B/-}$ mice and is an early hallmark of muscle pathogenesis and is indicative of impairment in muscle development (Boyer et al., unpublished). TSA is able to significantly decrease the proportion of centrally located nuclei in the *Smn*$^{2B/-}$ tibialis anterior muscle (**Figure 17B**). This finding is consistent with our findings of significantly fewer small caliber myofibers and more larger caliber myofibers in the TSA treated to *Smn*$^{2B/-}$ mice. Therefore, TSA has the ability to improve the maturity of myofibers. In the delta 7 model of SMA, TSA was able to improve the maturity of existing myofibers by affecting the myogenic regulatory program. TSA was able to increase the expression of myogenin and contractile filaments and lead to improvements in overall muscle maturity and motor behavior in this model of SMA (Avilla et al., 2007).

Smn$^{2B/-}$ *mice have a delay in the myogenic regulatory program*

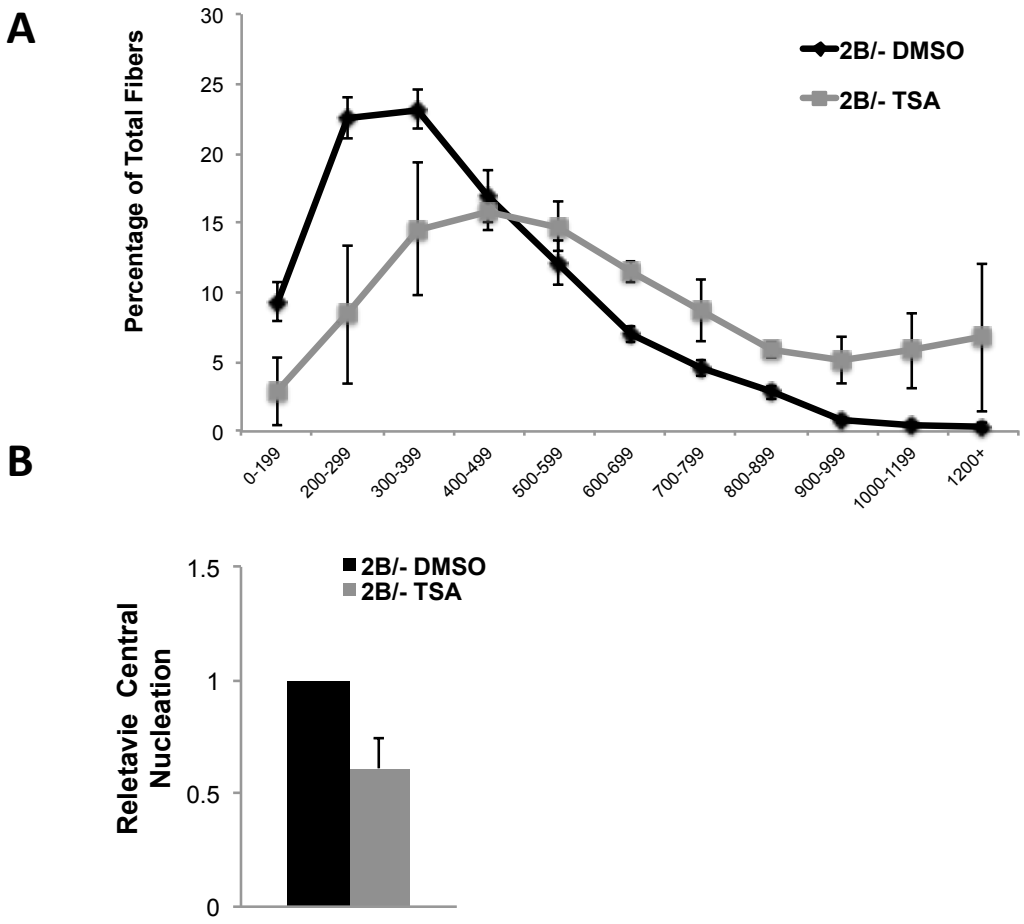

Figure 17. TSA treatment improves the maturity of TA muscle in *Smn*$^{2B/-}$ mice.

A) Graphical demonstration of significantly fewer small caliber fibers and an increased proportion of large caliber fibers in TA muscles of *Smn*$^{2B/-}$ mice following TSA treatment. There was a significant increase in myofiber size of TSA treated *Smn*$^{2B/-}$ mice compared with DMSO vehicle control**. B)** TSA is able to significantly decrease the proportion of centrally located nuclei in the *Smn*$^{2B/-}$ tibialis anterior muscle.

Our laboratory has recently identified a delay in the myogenic program in the *Smn*$^{2B/-}$ mice (Boyer et al., unpublished). In the early stages of development, the *Smn*$^{2B/-}$ have an abnormal myogenic regulatory program which persists into the later stages of the disease. This is supported both at the morphological level as evidenced by atrophy and presence of immature myofibers as well as at the molecular level by a misregulation of the myogenic program. The early myogenic regulatory factors Pax7 and MyoD are normally expressed at higher levels early in development to coordinate the formation of new muscle fibers and enhance growth. As this myogenic process continues, late myogenic regulatory factors such as myogenin start to be expressed to drive myogenesis and further develop functioning muscle. Late in development, the expression of these myogenic regulatory factors drops since there is no need for regeneration. Post muscle damage, muscle regeneration is quickly triggered and early myogenic regulatory factors turn on and shortly after the late myogenic regulatory factors drive the development process and complete the regeneration of functioning muscle. Early in the development of the *Smn*$^{2B/-}$ mice at postnatal day 2, the levels of the early myogenic regulatory factors such as Pax7 and MyoD are lower than wild type levels. Interestingly the levels of Pax7, MyoD, and myogenin are all higher than wild type later in development at P21 (Boyer et al., unpublished). The lower than normal expression early in development combined with the higher than normal expression late in development indicates that the *Smn*$^{2B/-}$ mice have a delay in the myogenic program. Furthermore, at our experimental endpoint for TSA injection on P25, the levels of Pax7, MyoD, and myogenin protein were all much higher than wild type levels (**Figure 18**). Normally at P25, the protein expression levels of Pax7, MyoD, and myogenin should be very low or almost undetectable. These results

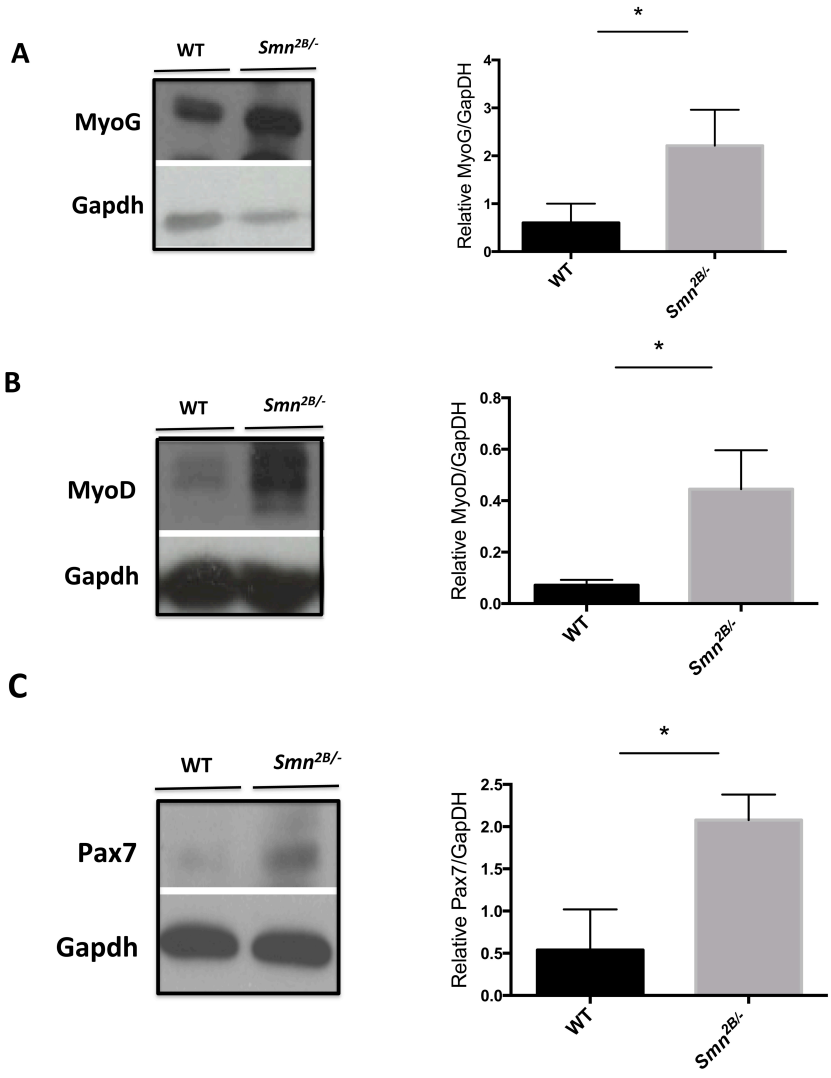

Figure 18. Hind limb muscles from *Smn*$^{2B/-}$ mice express higher levels of MyoD, MyoG, and Pax7 compared with wild type mice.

A) Western blot showing MyoD is expressed at a higher level in *Smn*$^{2B/-}$ mice at P25 compared to the wild type (WT) mice (n=3). **B)** Western blot showing *Smn*$^{2B/-}$ mice express higher levels of MyoG than wild type mice at P25 (n=3). **C)** Western blot showing *Smn*$^{2B/-}$ mice express higher levels of Pax7 than wild type mice at P25 (n=3).

indicate that muscle development is delayed in *Smn*$^{2B/-}$ mice.

TSA does not increase the protein levels of a late myogenic regulatory factor in the hind limb muscles of Smn$^{2B/-}$ *mice*

TSA has been shown to increase myogenin and levels of both perinatal and adult myosin heavy chain (MyHC) in the delta 7 mouse model of SMA (Avila et al., 2007). To further investigate the effects of TSA on SMA muscle, we measured the protein levels of myogenic regulatory factors that are misregulated in the *Smn*$^{2B/-}$ mice. The levels of Pax7, MyoD, and myogenin were already significantly increased at P25 in the untreated mice. Normally the levels of Pax7, MyoD, and myogenin are much lower at this stage in wild type mice. TSA was unable to further increase the protein levels of myogenin at P25 (**Figure 19B**). It is important to mention that while there was no further increase in myogenin protein levels, we observed an increase in the size of the myofiber. This phenotypically translated to improvements in motor behavior.

TSA increases the levels of early myogenic regulatory factors in the hind limb muscles of Smn$^{2B/-}$ *mice*

The levels of early myogenic regulatory factors such as Pax7 and MyoD are much higher at P25 in the *Smn*$^{2B/-}$ mice compared with wild type mice. TSA was able to further increase the protein levels of Pax7 and MyoD (**Figure 19A**). This further increase in the levels of Pax7 and MyoD indicate that TSA can enhance the muscle regeneration potential and satellite cell activation. This increase in the regeneration potential was

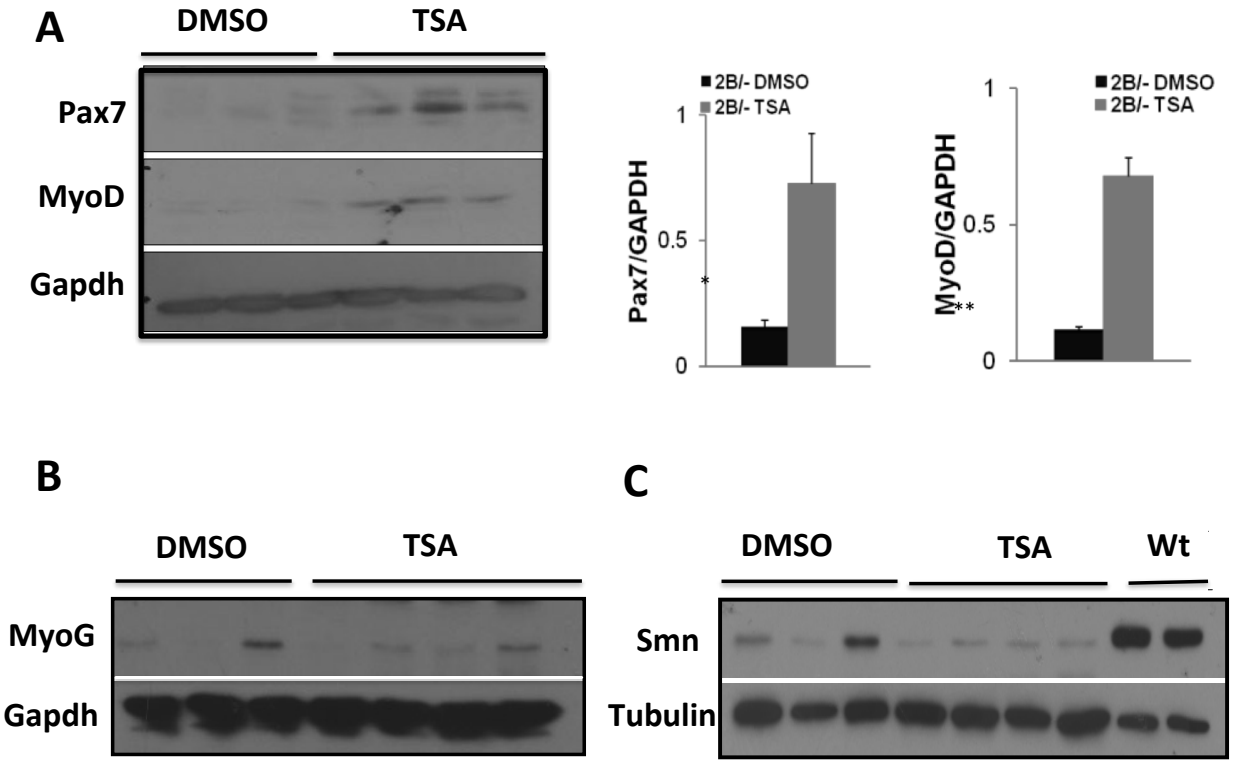

Figure 19. TSA increases MyoD and Pax7 expression levels in hind-limb muscle of *Smn*$^{2B/-}$ mice and has no impact on MyoG and Smn.

A) Western blot and quantification analysis showing that serial TSA injections increases MyoD and Pax7 levels in the hind limb muscle of P25 *Smn*$^{2B/-}$ mice (n=3). **B)** Western blot showing that serial TSA injection had no impact on late myogenic regulatory factor MyoG expression in hind limb muscle of P25 *Smn*$^{2B/-}$ mice (n=3). **C)** Western blot showing that serial TSA injections had no impact on Smn protein levels in hind limb

muscle of P25 *Smn*$^{2B/-}$ mice compared with DMSO treated mice (n=3). Samples from wild type mice served as positive control.

independent of Smn protein levels. Interestingly, our laboratory has recently shown that daily TSA injections in the *Smn*$^{2B/-}$ mice from P3-P6 can also increase the levels of Pax7 and MyoD (Boyer et al., unpublished). During this early stage of development, the *Smn*$^{2B/-}$ mice have a significant reduction in the expression levels of Pax7 and MyoD. Therefore, TSA is able to increase the levels of these early myogenic regulatory factors and enhance muscle development in an Smn-independent manner.

TSA increases the number of Pax7+ cells in the hind limb of Smn$^{2B/-}$ *mice*

TSA was able to increase the protein levels of Pax7. To investigate whether this corresponds to an increase in the number of satellite cells, we quantified the number of Pax7+ cells in the tibialis anterior muscle of *Smn*$^{2B/-}$ mice. We observed a significant increase in the number of satellite cells in the TA muscles of *Smn*$^{2B/-}$ mice (**Figure 20**). This increase in satellite cell number and the increase in the protein levels of Pax7 and MyoD indicate that TSA has regenerative potential in SMA muscle.

TSA improves overall muscle function independent of Smn levels

Taken together, our results indicate that TSA has the potential to improve muscle function and development. TSA was able to improve overall growth and lead to improvements in motor behavior. TSA treatment leads to histological improvements in the muscle and significantly improves myofiber size in the tibialis anterior muscle of *Smn*$^{2B/-}$ mice. TSA treatment also improved muscle development at the molecular level and enhanced the regeneration capacity as evident by the increase in the levels of myogenic regulatory factors that contribute to muscle development both early in

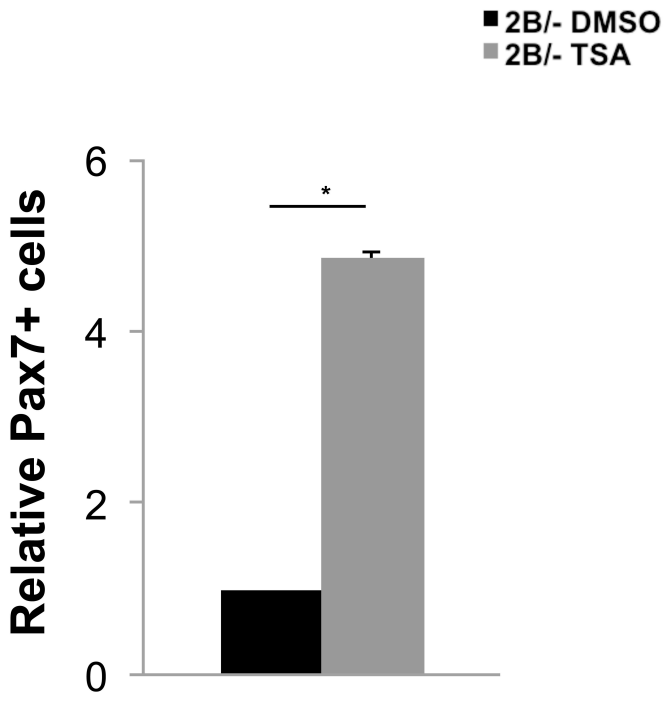

Figure 20. TSA increases the number of satellite cells in the tibialis anterior muscle. Histological analysis and staining using primary antibodies targeting Pax7 and laminin were used to highlight satellite cells and the basal lamina. A plot of relative number of Pax7 positive cells in the TSA and DMSO treated tibialis anterior (TA) muscle of $Smn^{2B/-}$ mice is shown. There is a significant increase in the number of satellite cells in the TSA treated group.

development as well as in later time points of the disease. Smn protein levels were not increased after TSA treatment in hindlimb muscles or primary myoblasts obtained from *Smn*$^{2B/-}$ mice. Therefore TSA has beneficial effects in the muscle of the *Smn*$^{2B/-}$ mice and most importantly these improvements are independent of SMN.

Discussion

Smn-independent therapeutic strategies can improve the SMA phenotype

There are several Smn-independent therapeutic strategies that produced promising results in mouse models of SMA. In these studies, there were clear phenotypic improvements in survival and motor function or other outcome measures regardless of changes in *Smn* transcript or protein levels. One of the consequences of *Smn*-depletion is overactivation of RhoA which is a major regulator of actin cytoskleton dynamics (Bowerman et al., 2010). Pharmacological inhibition of ROCK, a direct downstream effector of RhoA, can be achieved using Y-27632 or Fasudil. Treatment with Y-27632 leads to increased lifespan, improvement in the maturity of the NMJs, and increase in muscle fiber size independent of changes in Smn protein levels (Bowerman et al., 2010). Fasudil treatment had a similar effect and it was able to restore the normal expression of markers of skeletal muscle development, suggesting that the beneficial effects could be muscle-specific because no change in Smn protein levels or motor neuron number was identified (Bowerman et al., 2012). Another Smn-independent therapeutic approach targeting muscle that has increased the lifespan and myofiber size was through the overexpression of a local muscle isoform of IGF-1 in SMAΔ7 mice (Bosch-Marce et al., 2011). Furthermore, TSA in combination with the IGF-1 over-expression further extended survival and improved motor behavior however this combination was not

synergistic in the SMAΔ7 mice (Bosch-Marce et al., 2011). The myostatin/follistatin pathway has also been targeted as a muscle directed therapy, however the transgenic inactivation of myostatin, which is a negative regulator of muscle mass, does not confer any phenotypic improvements in SMA mice (Sumner et al., 2009; Rindt et al., 2011). Delivery of recombinant follistatin, which acts as an antagonist to myostatin, was able to increase survival, muscle mass, ventral horn cell number and size, and lead to improvements in motor function in a severe mouse model of SMA (Rose et al., 2008). Furthermore, these beneficial effects were independent of changes in Smn protein levels in the spinal cord or muscle (Rose et al., 2008). Therefore, various therapeutic avenues that have been successful in improving the SMA phenotype in mice work independently of *Smn*. Interestingly, survival and growth can be improved regardless of Smn protein levels in nervous or muscle tissue, or changes in motor neuron number.

TSA Improves the *Smn*$^{2B/-}$ phenotype independent of *Smn*

TSA has been shown to increase survival and motor behavior as well as increase Smn protein levels in the *SMN*Δ7 mouse model of SMA, which carries the human *SMN2* gene. The observed beneficial effects in the *SMN*Δ7 model was primarily attributed to the modest increase in Smn protein levels. Whether TSA confers its beneficial effects specifically and exclusively through increasing production of SMN or whether other genes respond to TSA has not been investigated before. Here, using the *Smn*$^{2B/-}$ mouse model of SMA, we have begun to address this question in more detail.

Since the *Smn*$^{2B/-}$ mouse model does not carry the human *SMN2* transgene, it could provide insight into the mechanism of action for TSA. Using daily IP injections of TSA from P12-25, we observed improvements in the phenotype of *Smn*$^{2B/-}$ mice. The improvement in general outcome measures such as survival, growth, and motor function clearly indicated a beneficial response. Particularly, there was a significant extension of lifespan. There was evidence of significant neuroprotection observed through a great reduction in the death of motor neurons in the ventral horn of the spinal cord. The increase in muscle fiber size and motor behavior are important outcome measures that show significant improvement in muscle of SMA model mice after TSA treatment. There was evidence of an increase in MyoD and Pax7 protein levels after TSA treatment, and an increase in the number of satellite cells in the TA muscle. The improvement in the maturity and size of the neuromuscular junction also provides further evidence that TSA improves various aspects of the phenotype. To investigate the molecular mechanism of the observed amelioration of phenotype, Smn protein and transcript levels were measured in various tissues and cells obtained from the *Smn*$^{2B/-}$ mouse. There was no significant increase in Smn protein levels after up to 500 nM of TSA treatment in mouse embryonic fibroblasts obtained from *Smn*$^{2B/-}$ mice. We observed no significant increase in Smn protein or transcript levels in the brain and spinal cord of the *Smn*$^{2B/-}$ mice. Furthermore, Smn protein levels did not increase in the hind limb muscle or primary myoblasts obtained from *Smn*$^{2B/-}$ mice. There was no increase in Smn protein levels in other vital organs such as the liver and heart of the *Smn*$^{2B/-}$ mice. These results demonstrate that the improvements observed in the SMA phenotype in the mice are primarily through an *Smn*-independent mechanism. Although Smn protein levels are not increased, TSA offers

general neuroprotection that is sufficient to extend survival and improve motor behavior and growth. Furthermore, TSA offers protection to motor neurons and has muscle regenerative capability as evident by an increase in satellite cell number.

HDAC inhibitors specifically increase expression from *SMN2*

It is important to emphasize that the spinal muscular atrophy cellular models, mouse models, and humans that were utilized in the previous studies all contain the human *SMN2* gene or transgene, and the reported increase in Smn protein levels are most likely exclusively through the activation of the *SMN2* promoter. VPA increases *SMN2* promoter activity as measured by beta-lactamase activity in NSC-34 cells in a dose dependent manner (Sumner et al., 2003). In another study, NSC-34 cells showed a dose dependent increase in promoter activity after treatment with SAHA and VPA (Kernochan et al., 2005). M344 is a pan-HDAC inhibitor similar to TSA, which is capable of correction of splicing and reverting delta 7 (Δ7) *SMN2* into full length *SMN2* through the elevation in the levels of human transformer-2-beta (Htra2-beta) in SMA patient fibroblasts (Riessland et al., 2006). LBH589 is another HDAC inhibitor that specifically increases *SMN2* transcript expression both in-vitro and in-vivo by increasing Htra2-beta as well as improving promoter access through H3K9 hyperacetylation (Garbes et al., 2009). TSA is a pan-HDAC inhibitor similar to SAHA and M344 and has been shown to increase *SMN2* activity in various in-vivo and in-vitro models including the SMAΔ7 model of SMA (Avilla et al., 2007; Jarecki et al., 2003; Kwon et al., 2011). There is little

evidence that the endogenous mouse *Smn* gene responds to HDAC inhibitors, specifically TSA. We showed that TSA does not increase murine Smn protein or transcript in various tissues and primary cells obtained from the $Smn^{2B/-}$ mice. Since this mouse model does not carry the human *SMN2* transgene and has a mutation in the endogenous murine *Smn* gene, we can conclude that the murine *Smn* gene does not respond to TSA.

Differential Regulation of *SMN2* by individual HDAC proteins

HDAC inhibitors can enhance the expression of *SMN2*. It is important to understand why the human *SMN2* responds to TSA and other HDAC inhibitors. It is important to identify specifically which HDAC proteins are important for inhibition to specifically target and enhance *SMN2* gene expression. The human *SMN1* and *SMN2* promoters are quasi-identical in sequence and share common regulatory elements with similar transcription regulation (Echaniz-Laguna et al., 1999), however differences exist that could lead to preferential expression of *SMN2* after TSA treatment. It must be emphasized that *SMN* regulatory sequences differ between the human and mouse *Smn* gene and can be as far as 4.6 kb upstream of the transcription initiation site (Kernochan et al., 2005). Another important point to consider is that HDACs have non-histone targets that are transcriptional regulators and TSA could exert its effect specifically on the *SMN2* gene through the activation of these regulators. Another point to consider is that TSA can inhibit class I and class II HDACs with relative potency which creates a pitfall. The non-specificity in inhibition creates the potential for various events which do not offer neuroprotection and may even be neurotoxic. The observation that $Smn^{2B/+}$ mice lose

weight following serial TSA administration indicates that TSA may have toxic effects under sufficient Smn levels. These off-target effects may be due to the non-specific inhibition of class I and II HDACs. Therefore it is important to address the individual HDACs responsible for increasing *SMN2*. Following identification of the responsible HDACs that are capable of increasing *SMN2,* specific inhibitors could be used to reduce the off targets pitfall of a pan HDAC inhibitor.

TSA improves the pathologic features of SMA in muscle independent of *Smn*

Several *Smn*-independent pathways have been identified in SMA muscle and therapeutic strategies have been successfully developed to target these pathways and yielded beneficial effects in SMA disease models. In the *SMN*Δ7 mouse model of SMA, TSA was able to increase the expression of myogenin, a late myogenic regulatory factor. The increase in myogenin corresponded to the increase in both the perinatal myosin heavy chain (MyHC) and of adult MyHC (Avila et al., 2007). Interestingly, the expression of early myogenic regulatory factors such as Pax7 and MyoD was unaltered by TSA treatment. Therefore, the enhanced synthesis of contractile filaments and increased maturity of muscle cells was the result of the increase in myogenin and all isoforms of MyHC, and not due to regeneration (Avila et al., 2007). Interestingly, in the $Smn^{2B/-}$ mouse model of SMA, there was an increase in protein levels of early but not late myogenic regulatory factors. TSA increased the protein levels of Pax7 and MyoD in hind limb muscles and increased the number of satellite cells in the TA muscle. TSA was

unable to increase the protein levels of Myogenin, unlike what was reported for the *SMN*Δ7 mouse model. Therefore, TSA can improve muscle regeneration in the $Smn^{2B/-}$ mice. It is critical to emphasize that these improvements are Smn-independent. Smn protein levels were not increased in the hind limb muscles or in the primary myoblasts obtained from the $Smn^{2B/-}$ mice. Therefore, serial TSA injections improve muscle regeneration and maturity independently of Smn protein levels and leads to histological improvements in myofiber size, which ultimately results improvement in growth and motor behavior.

TSA has neuroprotective effects independent of Smn

The $Smn^{2B/-}$ mouse model of SMA does not carry the human *SMN2* transgene and TSA is unable to increase Smn protein or transcript levels in the brain and spinal cord. However, there were clear signs of neuroprotection in these animals. The increase in the number of motor neurons in the lumbar spinal cord and improvements in the maturity of neuromuscular junctions observed in the TSA treated animals indicate that it has neuroprotective properties. The general observed benefit in terms of survival, growth, and motor behavior could also be partially attributed to the neuroprotective properties of TSA. HDAC inhibitors can have a wide range of targets for transcription initiation, however these are specific to the cell type or disease model, and vary according to several factors. TSA has general neuroprotective properties in various animal models and cellular conditions. TSA has protective properties in neurons by increasing alpha-synuclein levels

and protected against glutamate induced excitotoxicity in the cerebellum and frontal cortex as well as in cortical neurons (Leng and Chuang, 2006). Interestingly, oxidative stress and disturbed glutamate transport has been reported in type I SMA patients (Hayashi et al., 2002). TSA has neuroprotective properties by increasing cytoprotective HSP70 levels, and it concurrently suppresses P53 upregulation and can consequently inhibit the effects of this proapoptotic transcription factor (Kim et al., 2007). Other than playing a key role in neuroprotection, HSP70 also plays a role in the muscle and protects against the atrophic features also present in SMA (Miyabara et al., 2012). P53 does interact with Smn and the impairment in this interaction could lead to motor neuron apoptosis in SMA (Young et al., 2001). TSA also increases the levels of antiapoptotic Bcl-2 (Kim et al., 2007). Importantly, aberrant apoptosis through the down regulation of BCl-2 proteins in motor neurons of type I SMA patients is well documented (Soler-Botija et al., 2003). The increase in the number of spinal cord motor neurons in the *Smn*$^{2B/-}$ mice might potentially relate to the decrease in the apoptosis through antiapoptotic pathways such as these. Another important neuroprotective mechanism induced by TSA is the increase in neurotrophic support to existing neurons. TSA can robustly increase the levels of BDNF and GDNF by increasing promoter activity and can provide trophic support to the surviving motor neurons (Wu et al., 2008). TSA was able to increase BDNF transcript levels in the *Smn*$^{2B/-}$ mice (Unpublished data, Dr. Hong Liu). and this increase could contribute to the survival of motor neurons. It should be emphasized that other HDAC inhibitors are known to be involved in other neuroprotective pathways, and TSA could also lead to improvements in the intermediate SMA mouse model through those pathways. The temporal effects of TSA must also be considered. The neuroprotective

mechanisms and pathways that TSA utilizes are different in adults compared with neonates in a stroke model and interestingly not through the common neuroprotective mechanisms suggested previously in stroke disease models (Fleiss et al., 2012). To assess which neuroprotective pathways are involved in the *Smn*$^{2B/-}$ intermediate mouse model of SMA, a microarray approach is an appropriate route. Since TSA causes changes in the expression of many genes, it is hard to individually approach these pathways and a broad overview of these pathways could lead to insight into how TSA provides cumulative neuroprotection.

The future role of TSA in SMA therapeutics

Although the initial set of experiments using HDAC inhibitors in animal models and human SMA patient cell lines were promising and demonstrated significant improvements, in human clinical trials they did not show any signs of significant benefit. Although these HDAC inhibitors failed to demonstrate signs of efficacy, there were select patients that showed signs of improvement after treatment with HDAC inhibitors. TSA was not tested in human clinical trials for SMA and it is not known if this drug would be capable to improve the human phenotype. It is more likely that TSA will not reach the stage of clinical trials due to the failure of other HDAC inhibitors to lead to phenotypic improvements in human patients. What is more likely to occur with TSA is the identification of new therapeutic targets that may be Smn-independent. In the *Smn*$^{2B/-}$ mouse model of SMA, TSA was unable to increase *Smn* transcript and protein levels yet the animals were significantly healthier than their DMSO recipient littermates. This indicates that TSA can be neuroprotective in an Smn-independent manner and

identification of those *SMN*-independent pathways could lead to the discovery of new drugs that can benefit SMA patients.

Conclusion

TSA, a potent pan-HDAC inhibitor was able to significantly improve the phenotype caused by Smn deficiency in the *Smn*$^{2B/-}$ intermediate mouse model of SMA. TSA crossed the blood brain barrier and was well tolerated by the *Smn*$^{2B/-}$ mice. TSA treated *Smn*$^{2B/-}$ mice were significantly better on outcome measures such as survival, growth, motor behavior, motor neuron survival, neuromuscular junction maturity, muscle histology, and muscle development. To examine the mechanisms involved and responsible for the beneficial outcomes observed in *Smn*$^{2B/-}$ mice, we measured Smn protein and mRNA transcript levels in various cells and tissues obtained from *Smn*$^{2B/-}$ mice. TSA was unable to increase Smn protein levels in mouse embryonic fibroblasts or myoblasts obtained from the *Smn*$^{2B/-}$ mice. TSA was unable to increase *Smn* transcript levels in the brain and spinal cord of *Smn*$^{2B/-}$ mice. Furthermore, TSA did not increase Smn protein levels in the brain, spinal cord, hind limb muscle, heart muscle, or the liver of *Smn*$^{2B/-}$ mice. Therefore, the beneficial effects observed in this study are likely through an Smn-independent pathway. Rather than a specific increase in Smn levels, TSA likely causes global transcriptional changes and orchestrates the activity of meuroprotective and regenerative pathways that improve the phenotype in *Smn*$^{2B/-}$ mice. A microarray approach could be used to identify the exact combination of neuroprotective pathways that are responsive to TSA. Treatment with TSA improved myofiber size and increased the activity of several myogenic regulatory factors involved in muscle development and regeneration. This increase was independent of changes in Smn protein levels in the hind limb muscle or primary myoblasts obtained from *Smn*$^{2B/-}$ mice. Therefore, the beneficial effects of TSA are likely through Smn-independent pathways and identifying and

targeting these pathways could lead to the development of novel therapeutics in the fight against SMA.

References:

Andreassi, Catia; Angelozzi, Carla; Tiziano, Francesco D; et al. (2004): „Phenylbutyrate increases SMN expression in vitro: relevance for treatment of spinal muscular atrophy.“. In: *European journal of human genetics : EJHG*. 12 , pp. 59–65, DOI: 10.1038/sj.ejhg.5201102. — ISBN: 1018-4813 (Print)r1018-4813 (Linking)

Avila, Amy M; Burnett, Barrington G; Taye, Addis A; et al. (2007): „Trichostatin A increases SMN expression and survival in a mouse model of spinal muscular atrophy.“. In: *The Journal of clinical investigation*. 117 , pp. 659–671, DOI: 10.1172/JCI29562. — ISBN: 0021-9738 (Print)

Azzouz, M; Le, T; Ralph, G S; et al. (2004): „Lentivector-mediated SMN replacement in a mouse model of spinal muscular atrophy“. In: *J. Clin. Invest*. 114 , pp. 1726–1731, DOI: 10.1172/JCI22922. — ISBN: 0021-9738 (Print)

Van Bergeijk, Jeroen; Haastert, Kirsten; Grothe, Claudia; et al. (2006): „Valproic acid promotes neurite outgrowth in PC12 cells independent from regulation of the survival of motoneuron protein.“. In: *Chemical biology & drug design*. 67 , pp. 244–247, DOI: 10.1111/j.1747-0285.2006.00369.x. — ISBN: 1747-0277 (Print)r1747-0277 (Linking)

Bosch-Marcé, Marta; Wee, Claribel D; Martinez, Tara L; et al. (2011): „Increased IGF-1 in muscle modulates the phenotype of severe SMA mice.“. In: *Human molecular genetics*. 20 , pp. 1844–1853, DOI: 10.1093/hmg/ddr067.

Boutillier, Anne-Laurence; Trinh, Emmanuelle; Loeffler, Jean-Philippe (2003): „Selective E2F-dependent gene transcription is controlled by histone deacetylase activity during neuronal apoptosis.“. In: *Journal of neurochemistry*. 84 , pp. 814–828, DOI: 1581 [pii]. — ISBN: 0022-3042 (Print)

Bowerman, Mélissa; Anderson, Carrie L; Beauvais, Ariane; et al. (2009): „SMN, profilin IIa and plastin 3: a link between the deregulation of actin dynamics and SMA pathogenesis.“. In: *Molecular and cellular neurosciences*. 42 , pp. 66–74, DOI: 10.1016/j.mcn.2009.05.009. — ISBN: 1095-9327 (Electronic)r1044-7431 (Linking)

Bowerman, Mélissa; Beauvais, Ariane; Anderson, Carrie L; et al. (2010): „Rho-kinase inactivation prolongs survival of an intermediate SMA mouse model.“. In: *Human molecular genetics*. 19 , pp. 1468–1478, DOI: 10.1093/hmg/ddq021.

Bowerman, Melissa; Murray, Lyndsay M; Boyer, Justin G; et al. (2012a): „Fasudil improves survival and promotes skeletal muscle development in a mouse model of spinal muscular atrophy.“. In: *BMC medicine*. 10 , p. 24, DOI: 10.1186/1741-7015-10-24.

Bowerman, Melissa; Swoboda, Kathryn J; Michalski, John-Paul; et al. (2012b): „Glucose metabolism and pancreatic defects in spinal muscular atrophy.“. In: *Annals of neurology*. 72 , pp. 256–68, DOI: 10.1002/ana.23582.

Boyer, Justin G; Murray, Lyndsay M; Scott, Kyle; et al. (2013): „Early onset muscle weakness and disruption of muscle proteins in mouse models of spinal muscular atrophy.“. In: *Skeletal muscle*. 3 , p. 24, DOI: 10.1186/2044-5040-3-24.

Brichta, L; Hofmann, Y; Hahnen, E; et al. (2003): „Valproic acid increases the SMN2 protein level: a well-known drug as a potential therapy for spinal muscular atrophy.“. In: *Human molecular genetics*. 12 , pp. 2481–2489, DOI: 10.1093/hmg/ddg256. — ISBN: 0964-6906 (Print)r0964-6906 (Linking)

Chang, J G; Hsieh-Li, H M; Jong, Y J; et al. (2001): „Treatment of spinal muscular atrophy by sodium butyrate“. In: *Proc Natl Acad Sci U S A*. 98 , pp. 9808–9813, DOI: 10.1073/pnas.171105098\r98/17/9808 [pii]. — ISBN: 0027-8424 (Print)r0027-8424 (Linking)

Cho, Sungchan; Dreyfuss, Gideon (2010): „A degron created by SMN2 exon 7 skipping is a principal contributor to spinal muscular atrophy severity.“. In: *Genes & development*. 24 , pp. 438–442, DOI: 10.1101/gad.1884910. — ISBN: 1549-5477 (Electronic)r0890-9369 (Linking)

Chuang, De-Maw; Leng, Yan; Marinova, Zoya; et al. (2009): „Multiple roles of HDAC inhibition in neurodegenerative conditions.“. In: *Trends in neurosciences*. 32 , pp. 591–601, DOI: 10.1016/j.tins.2009.06.002. — ISBN: 1878-108X (Electronic)r0166-2236 (Linking)

Cifuentes-Diaz, C; Frugier, T; Tiziano, F D; et al. (2001): „Deletion of murine SMN exon 7 directed to skeletal muscle leads to severe muscular dystrophy.“. In: *The Journal of cell biology*. 152 , pp. 1107–1114, DOI: 10.1083/jcb.152.5.1107. — ISBN: 0021-9525 (Print)

Consortium, S M A; Of, Report (1993): „(26-28 June 1992, Bonn, Germany)“. In: *Neuromuscul Disord*. 2 (5), pp. 423–428.

Crawford, T O; Pardo, C a (1996): „The neurobiology of childhood spinal muscular atrophy.“. In: *Neurobiology of disease*. 3 (2), pp. 97–110, DOI: 10.1006/nbdi.1996.0010.

deTombe, Pieter P.; Miyabara, Elen H.; Mestril, Ruben; et al. (2012): „Overexpression of inducible 70-kDa heat shock protein in mouse improves structural and functional recovery of skeletal muscles from atrophy“. *Pflügers Archiv - European Journal of Physiology*., DOI: 10.1007/s00424-012-1087-x.

DiDonato, C J; Chen, X N; Noya, D; et al. (1997): „Cloning, characterization, and copy number of the murine survival motor neuron gene: homolog of the spinal muscular atrophy-determining gene.“. In: *Genome research*. 7 , pp. 339–352, DOI: 10.1101/gr.7.4.339. — ISBN: 1088-9051 (Print)

DiDonato, C J; Lorson, C L; De Repentigny, Y; et al. (2001): „Regulation of murine survival motor neuron (Smn) protein levels by modifying Smn exon 7 splicing.“. In: *Human molecular genetics*. 10 , pp. 2727–2736. — ISBN: 0964-6906 (Print)r0964-6906 (Linking)

Dubowitz, V (1999): „Very severe spinal muscular atrophy (SMA type 0): an expanding clinical phenotype.“. In: *European journal of paediatric neurology : EJPN : official journal of the European Paediatric Neurology Society*. 3 (2), pp. 49–51, DOI: 10.1053/ejpn.1999.0181.

Echaniz-Laguna, A; Miniou, P; Bartholdi, D; et al. (1999): „The promoters of the survival motor neuron gene (SMN) and its copy (SMNc) share common regulatory elements.“. In: *American journal of human genetics*. 64 , pp. 1365–1370, DOI: 10.1086/302372. — ISBN: 0002-9297 (Print)r0002-9297 (Linking)

Faraco, Giuseppe; Cavone, Leonardo; Chiarugi, Alberto (2011): „The therapeutic potential of HDAC inhibitors in the treatment of multiple sclerosis.“. In: *Molecular medicine (Cambridge, Mass.)*. 17 , pp. 442–7, DOI: 10.2119/molmed.2011.00077.

Feldkötter, Markus; Schwarzer, Verena; Wirth, Radu; et al. (2002): „Quantitative analyses of SMN1 and SMN2 based on real-time lightCycler PCR: fast and highly reliable carrier testing and prediction of severity of spinal muscular atrophy.“. In: *American journal of human genetics*. 70 , pp. 358–368, DOI: 10.1086/338627. — ISBN: 0002-9297 (Print)

Finazzi, Guido; Rambaldi, Alessandro; Leoni, Flavio; et al. (2012): „Givinostat and Hydroxyurea synergize in vitro to induce apoptosis of cells from JAK2V617F Myeloproliferative Neoplasm patients“. *Experimental Hematology*., DOI: 10.1016/j.exphem.2012.10.013.

Fischer, U; Liu, Q; Dreyfuss, G (1997): „The SMN-SIP1 complex has an essential role in spliceosomal snRNP biogenesis.“. In: *Cell*. 90 , pp. 1023–1029, DOI: 10.1016/S0092-8674(00)80368-2. — ISBN: 0092-8674 (Print)

Fleiss, Bobbi; Blomgren, Klas; Nilsson, Marie KL; et al. (2012): „Neuroprotection by the histone deacetylase inhibitor trichostatin A in a model of lipopolysaccharide-sensitised neonatal hypoxic-ischaemic brain injury“. *Journal of Neuroinflammation*., DOI: 10.1186/1742-2094-9-70. — ISBN: 1742-2094 (Electronic)r1742-2094 (Linking)

Foust, Kevin D; Wang, Xueyong; McGovern, Vicki L; et al. (2010): „Rescue of the spinal muscular atrophy phenotype in a mouse model by early postnatal delivery of SMN.“. In: *Nature biotechnology*. 28 , pp. 271–274, DOI: 10.1038/nbt.1610. — ISBN: 1546-1696 (Electronic)n1087-0156 (Linking)

Garbes, Lutz; Riessland, Markus; Hölker, Irmgard; et al. (2009): „LBH589 induces up to 10-fold SMN protein levels by several independent mechanisms and is effective even in cells from SMA patients non-responsive to valproate.“. In: *Human molecular genetics*. 18 , pp. 3645–3658, DOI: 10.1093/hmg/ddp313. — ISBN: 2214788646

Gardian, Gabriella; Browne, Susan E; Choi, Dong-Kug; et al. (2005): „Neuroprotective effects of phenylbutyrate in the N171-82Q transgenic mouse model of Huntington's disease.“. In: *The Journal of biological chemistry*. 280 , pp. 556–563, DOI: 10.1074/jbc.M410210200.

Granger, Anne; Abdullah, Ibrahim; Huebner, Faith; et al. (2008): „Histone deacetylase inhibition reduces myocardial ischemia-reperfusion injury in mice“. In: *The FASEB Journal*. 22 , pp. 3549–3560, DOI: 10.1096/fj.08-108548.

Greenfield, J. G. , Shy, G. M. , Alvord, E. C. , and Berg, L. (1957): „An Atlas of Muscle Pathology in Neuromuscular Diseases“. Edinburgh: E. and S. Livingstone.

Hahnen, E; Hauke, J; Trankle, C; et al. (2008): „Histone deacetylase inhibitors: possible implications for neurodegenerative disorders“. In: *Expert Opin Investig Drugs*. 17 , pp. 169–184, DOI: 10.1517/13543784.17.2.169. — ISBN: 1744-7658 (Electronic)r1354-3784 (Linking)

Hahnen, Eric; Eyüpoglu, Ilker Y; Brichta, Lars; et al. (2006): „In vitro and ex vivo evaluation of second-generation histone deacetylase inhibitors for the treatment of spinal muscular atrophy.“. In: *J Neurochem*. 98 , pp. 193–202, DOI: 10.1111/j.1471-4159.2006.03868.x.

Hammond, Suzan M; Gogliotti, Rocky G; Rao, Vamshi; et al. (2010): „Mouse survival motor neuron alleles that mimic SMN2 splicing and are inducible rescue embryonic lethality early in development but not late.“. In: *PloS one*. 5 , p. e15887, DOI: 10.1371/journal.pone.0015887.

Harahap, Indra Sari Kusuma; Morikawa, Satoru; Nishimura, Noriyuki; et al. (2012): „Valproic acid increases SMN2 expression and modulates SF2/ASF and hnRNPA1 expression in SMA fibroblast cell lines“. *Brain and Development*., DOI: 10.1016/j.braindev.2011.04.010. — ISBN: 1872-7131 (Electronic)n0387-7604 (Linking)

Hausmanowa-Petrusewicz, I; Zaremba, J; Borkowska, J; et al. (1984): „Chronic proximal spinal muscular atrophy of childhood and adolescence: sex influence.“. In: *Journal of medical genetics*. 21 (6), pp. 447–50.

Hayashi, M; Araki, S; Arai, N; et al. (2002): „Oxidative stress and disturbed glutamate transport in spinal muscular atrophy“. In: *Brain Dev*. 24 , pp. 770–775, DOI: S0387760402001031 [pii]. — ISBN: 0387-7604 (Print)r0387-7604 (Linking)

Hockly, Emma; Richon, Victoria; Woodman, Benjamin; et al. (2003): „Suberoylanilide hydroxamic acid, a histone deacetylase inhibitor, ameliorates motor deficits in a mouse model of Huntington's disease.“. In: *Proceedings of the National Academy of Sciences of the United States of America*. 100 , pp. 2041–2046.

Hubbert, Charlotte; Guardiola, Amaris; Shao, Rong; et al. (2002): „HDAC6 is a microtubule-associated deacetylase.“. In: *Nature*. 417 , pp. 455–458, DOI: 10.1038/417455a. — ISBN: 0028-0836 (Print)r0028-0836 (Linking)

Jarecki, Jill; Chen, Xiaocun; Bernardino, Alexandra; et al. (2005): „Diverse small-molecule modulators of SMN expression found by high-throughput compound screening: early leads towards a therapeutic for spinal muscular atrophy.“. In: *Human molecular genetics*. 14 , pp. 2003–2018, DOI: 10.1093/hmg/ddi205. — ISBN: 0964-6906 (Print)

Kernochan, Lauren E; Russo, Melissa L; Woodling, Nathaniel S; et al. (2005): „The role of histone acetylation in SMN gene expression.“. In: *Human molecular genetics*. 14 , pp. 1171–1182, DOI: 10.1093/hmg/ddi130.

Kilgore, Mark; Miller, Courtney A; Fass, Daniel M; et al. (2010): „Inhibitors of class 1 histone deacetylases reverse contextual memory deficits in a mouse model of Alzheimer's disease.“. In: *Neuropsychopharmacology : official publication of the American College of Neuropsychopharmacology*. 35 , pp. 870–880, DOI: 10.1038/npp.2009.197. — ISBN: 1740-634X (Electronic)r0006-3223 (Linking)

Kim, Hyeon Ju; Rowe, Michael; Ren, Ming; et al. (2007): „Histone deacetylase inhibitors exhibit anti-inflammatory and neuroprotective effects in a rat permanent ischemic model of stroke: multiple mechanisms of action.“. In: *The Journal of pharmacology and experimental therapeutics*. 321 , pp. 892–901, DOI: 10.1124/jpet.107.120188. — ISBN: 0022-3565

Kissel, John T; Elsheikh, Bakri; King, Wendy M; et al. (2013): „SMA VALIANT Trial: A prospective, double-blind, placebo controlled trial of valproic acid in ambulatory adults with spinal muscular atrophy.“. In: *Muscle Nerve*., DOI: 10.1002/mus.23904.

Kissel, John T; Scott, Charles B; Reyna, Sandra P; et al. (2011): „SMA CARNIVAL TRIAL PART II: a prospective, single-armed trial of L-carnitine and valproic acid in ambulatory children with spinal muscular atrophy.“. In: *PloS one*. 6 , p. e21296, DOI: 10.1371/journal.pone.0021296. — ISBN: 1932-6203 (Electronic)r1932-6203 (Linking)

Kolb, Stephen J; Kissel, John T (2011): „Spinal muscular atrophy: a timely review.“. In: *Archives of neurology*. 68 (8), pp. 979–84, DOI: 10.1001/archneurol.2011.74.

Kwon, Deborah Y; Motley, William W; Fischbeck, Kenneth H; et al. (2011): „Increasing expression and decreasing degradation of SMN ameliorate the spinal muscular atrophy phenotype in mice.“. In: *Human molecular genetics*. 20 , pp. 3667–3677, DOI: 10.1093/hmg/ddr288.

Le, Thanh T; McGovern, Vicki L; Alwine, Isaac E; et al. (2011): „Temporal requirement for high SMN expression in SMA mice.“. In: *Human molecular genetics*. 20 , pp. 3578–3591, DOI: 10.1093/hmg/ddr275.

Le, Thanh T; Pham, Lan T; Butchbach, Matthew E R; et al. (2005): „SMNDelta7, the major product of the centromeric survival motor neuron (SMN2) gene, extends survival in mice with spinal muscular atrophy and associates with full-length SMN.“. In: *Human molecular genetics*. 14 , pp. 845–857, DOI: 10.1093/hmg/ddi078. — ISBN: 0964-6906 (Print)

Lefebvre, S; Bürglen, L; Reboullet, Sophie (1995): „Identification and characterization of a spinal muscular atrophy-determining gene“. In: *Cell*. 80 , pp. 155–165.

Lefebvre, S; Burlet, P; Liu, Q; et al. (1997): „Correlation between severity and SMN protein level in spinal muscular atrophy.“. In: *Nature genetics*. 16 , pp. 265–269, DOI: 10.1038/ng0797-265. — ISBN: 1061-4036 (Print)r1061-4036 (Linking)

Leng, Yan; Chuang, De-Maw (2006): „Endogenous alpha-synuclein is induced by valproic acid through histone deacetylase inhibition and participates in neuroprotection against glutamate-induced excitotoxicity.“. In: *The Journal of neuroscience : the official journal of the Society for Neuroscience*. 26 , pp. 7502–7512, DOI: 10.1523/JNEUROSCI.0096-06.2006. — ISBN: 1529-2401 (Electronic)r0270-6474 (Linking)

Liu, Hong; Shafey, Dina; Moores, Justin N; et al. (2010): „Neurodevelopmental consequences of Smn depletion in a mouse model of spinal muscular atrophy.“. In: *Journal of neuroscience research*. 88 , pp. 111–122, DOI: 10.1002/jnr.22189. — ISBN: 1097-4547 (Electronic)r0360-4012 (Linking)

Liu, Q; Dreyfuss, G (1996): „A novel nuclear structure containing the survival of motor neurons protein.“. In: *The EMBO journal*. 15 , pp. 3555–3565.

Lorson, C L; Hahnen, E; Androphy, E J; et al. (1999): „A single nucleotide in the SMN gene regulates splicing and is responsible for spinal muscular atrophy.“. In: *Proceedings of the National Academy of Sciences of the United States of America*. 96 , pp. 6307–6311, DOI: 10.1073/pnas.96.11.6307. — ISBN: 0027-8424 (Print)r0027-8424 (Linking)

Lotti, Francesco; Beck, Erin S.; Mentis, George Z.; et al. (2012): „An SMN-Dependent U12 Splicing Event Essential for Motor Circuit Function“. *Cell*., DOI: 10.1016/j.cell.2012.09.012. — ISBN: 1097-4172 (Electronic)r0092-8674 (Linking)

McKeran, R O; Ward, P; Slavin, G; et al. (1979): „Central nuclear counts in muscle fibres before and during treatment in hypothyroid myopathy.“. In: *Journal of clinical pathology*. 32 , pp. 229–233, DOI: 10.1136/jcp.32.3.229.

Mercuri, E; Bertini, E; Messina, S; et al. (2007): *Randomized, double-blind, placebo-controlled trial of phenylbutyrate in spinal muscular atrophy*. *Neurology*., DOI: 10.1212/01.wnl.0000249142.82285.d6. — ISBN: 1526-632X (Electronic)

Mishra, Nilamadhab; Reilly, Christopher M; Brown, Doris R; et al. (2003): „Histone deacetylase inhibitors modulate renal disease in the MRL-lpr/lpr mouse.“. In: *The Journal of clinical investigation*. 111 , pp. 539–552, DOI: 10.1172/JCI200316153. — ISBN: 0021-9738 (Print)

Monani, U R; Lorson, C L; Parsons, D W; et al. (1999): „A single nucleotide difference that alters splicing patterns distinguishes the SMA gene SMN1 from the copy gene SMN2.“. In: *Human molecular genetics*. 8 , pp. 1177–1183, DOI: 10.1093/hmg/8.7.1177. — ISBN: 0964-6906 (Print)r0964-6906 (Linking)

Monani, U R; Sendtner, M; Coovert, D D; et al. (2000): „The human centromeric survival motor neuron gene (SMN2) rescues embryonic lethality in Smn(-/-) mice and results in a mouse with spinal

muscular atrophy.“. In: *Human molecular genetics*. 9 , pp. 333–339, DOI: 10.1093/hmg/ddm236. — ISBN: 0964-6906 (Print)r0964-6906 (Linking)

Monneret, C (2007): „Histone deacetylase inhibitors for epigenetic therapy of cancer“. In: *Anticancer Drugs*. 18 , pp. 363–70., DOI: 10.1097/CAD.0b013e328012a5db. — ISBN: 0959-4973 (Print)

Murray, Lyndsay M; Comley, Laura H; Thomson, Derek; et al. (2008): „Selective vulnerability of motor neurons and dissociation of pre- and post-synaptic pathology at the neuromuscular junction in mouse models of spinal muscular atrophy.“. In: *Human molecular genetics*. 17 , pp. 949–962, DOI: 10.1093/hmg/ddm367. — ISBN: 1460-2083 (Electronic)r0964-6906 (Linking)

Murray, Lyndsay M.; Bowerman, Mélissa; Pinheiro, Bruno; et al. (2012): „A critical smn threshold in mice dictates onset of an intermediate spinal muscular atrophy phenotype associated with a distinct neuromuscular junction pathology“. *Neuromuscular Disorders*., DOI: 10.1016/j.nmd.2011.09.007.

Mutsaers, Chantal A; Wishart, Thomas M; Lamont, Douglas J; et al. (2011): „Reversible molecular pathology of skeletal muscle in spinal muscular atrophy.“. In: *Hum Mol Genet*. 20 , pp. 4334–44, DOI: 10.1093/hmg/ddr360.

Narver, Heather L; Kong, Lingling; Burnett, Barrington G; et al. (2008): „Sustained improvement of spinal muscular atrophy mice treated with trichostatin A plus nutrition.“. In: *Annals of neurology*. 64 , pp. 465–470, DOI: 10.1002/ana.21449. — ISBN: 1531-8249 (Electronic)

Oskoui, M; Levy, G; Garland, C J; et al. (2007): „The changing natural history of spinal muscular atrophy type 1.“. In: *Neurology*. 69 , pp. 1931–1936, DOI: 10.1212/01.wnl.0000290830.40544.b9. — ISBN: 0028-3878

Passini, M A; Bu, J; Roskelley, E M; et al. (2010): „CNS-targeted gene therapy improves survival and motor function in a mouse model of spinal muscular atrophy“. In: *J Clin Invest*. 120 , pp. 1253–1264, DOI: 41615 [pii]\n10.1172/JCI41615. — ISBN: 1558-8238 (Electronic)n0021-9738 (Linking)

Pearn, John (1978): „qequency studies of chronic childhood spinal muscular atrophy“. In: *J Med Genet*., pp. 409–413.

Piepers, Sanne; Cobben, Jan-Maarten; Sodaar, Peter; et al. (2011): „Quantification of SMN protein in leucocytes from spinal muscular atrophy patients: effects of treatment with valproic acid.“. In: *Journal of neurology, neurosurgery, and psychiatry*. 82 , pp. 850–852, DOI: 10.1136/jnnp.2009.200253. — ISBN: 1468-330X (Electronic)r0022-3050 (Linking)

Rak, Kristen; Lechner, Barbara Dorothea; Schneider, Christine; et al. (2009): „Valproic acid blocks excitability in SMA type I mouse motor neurons.“. In: *Neurobiology of disease*. 36 , pp. 477–487, DOI: 10.1016/j.nbd.2009.08.014. — ISBN: 1095-953X (Electronic)r0969-9961 (Linking)

Riessland, Markus; Ackermann, Bastian; Förster, Anja; et al. (2010): „SAHA ameliorates the SMA phenotype in two mouse models for spinal muscular atrophy.“. In: *Human molecular genetics*. 19 , pp. 1492–1506, DOI: 10.1093/hmg/ddq023. — ISBN: 2214788646

Riessland, Markus; Brichta, Lars; Hahnen, Eric; et al. (2006): „The benzamide M344, a novel histone deacetylase inhibitor, significantly increases SMN2 RNA/protein levels in spinal muscular atrophy cells.“. In: *Human genetics*. 120 , pp. 101–110, DOI: 10.1007/s00439-006-0186-1. — ISBN: 0043900601861

Rose, Ferrill F; Mattis, Virginia B; Rindt, Hansjörg; et al. (2009): „Delivery of recombinant follistatin lessens disease severity in a mouse model of spinal muscular atrophy.“. In: *Human molecular genetics*. 18 , pp. 997–1005, DOI: 10.1093/hmg/ddn426. — ISBN: 5738842219

Rouaux, Caroline; Jokic, Natasa; Mbebi, Corinne; et al. (2003): „Critical loss of CBP/p300 histone acetylase activity by caspase-6 during neurodegeneration.“. In: *The EMBO journal*. 22 , pp. 6537–6549, DOI: 10.1093/emboj/cdg615. — ISBN: 0261-4189 (Print)

Ryu, Hoon; Smith, Karen; Camelo, Sandra I; et al. (2005): „Sodium phenylbutyrate prolongs survival and regulates expression of anti-apoptotic genes in transgenic amyotrophic lateral sclerosis mice.“. In: *Journal of neurochemistry*. 93 , pp. 1087–1098, DOI: 10.1111/j.1471-4159.2005.03077.x. — ISBN: 0022-3042 (Print)r0022-3042 (Linking)

Saha, R N; Pahan, K (2006): „HATs and HDACs in neurodegeneration: a tale of disconcerted acetylation homeostasis.“. In: *Cell death and differentiation*. 13 , pp. 539–550, DOI: 10.1038/sj.cdd.4401769. — ISBN: 1350-9047

Sanderson, L; Taylor, G W; Aboagye, E O; et al. (2004): „Plasma pharmacokinetics and metabolism of the histone deacetylase inhibitor trichostatin a after intraperitoneal administration to mice.“. In: *Drug metabolism and disposition: the biological fate of chemicals*. 32 , pp. 1132–1138, DOI: 10.1124/dmd.104.000638. — ISBN: 0090-9556 (Print)

Schrank, Bertold; Götz, Rudolf; Gunnersen, Jennifer M.; et al. (1997): „Inactivation of the survival motor neuron gene, a candidate gene for human spinal muscular atrophy, leads to massive cell death in early mouse embryos“. In: *Proceedings of the National Academy of Sciences of the United States of America*. 94 , pp. 9920–9925.

Schreml, Julia; Garbes, Lutz; Parson, Simon H; et al. (2012): „Severe SMA mice show organ impairment that cannot be rescued by therapy with the HDACi JNJ-26481585“. *European Journal of Human Genetics*., DOI: 10.1038/ejhg.2012.222.

Shababi, Monir; Habibi, Javad; Yang, Hsiao T; et al. (2010): „Cardiac defects contribute to the pathology of spinal muscular atrophy models.“. In: *Human molecular genetics*. 19 , pp. 4059–4071, DOI: 10.1093/hmg/ddq329. — ISBN: 5738842219

Shafey, Dina; Côté, Patrice D; Kothary, Rashmi (2005): „Hypomorphic Smn knockdown C2C12 myoblasts reveal intrinsic defects in myoblast fusion and myotube morphology.“. In: *Experimental cell research*. 311 , pp. 49–61, DOI: 10.1016/j.yexcr.2005.08.019. — ISBN: 0014-4827 (Print)r0014-4827 (Linking)

Soler-Botija, Carolina; Ferrer, Isidro; Alvarez, Jose Luis; et al. (2003): „Downregulation of Bcl-2 proteins in type I spinal muscular atrophy motor neurons during fetal development.“. In: *Journal of neuropathology and experimental neurology*. 62 , pp. 420–426. — ISBN: 0022-3069 (Print)r0022-3069 (Linking)

Steffan, J S; Kazantsev, A; Spasic-Boskovic, O; et al. (2000): „The Huntington's disease protein interacts with p53 and CREB-binding protein and represses transcription.“. In: *Proceedings of the National Academy of Sciences of the United States of America*. 97 , pp. 6763–6768, DOI: 10.1073/pnas.100110097. — ISBN: 0027-8424 (Print)n0027-8424 (Linking)

Sugarman, Elaine a; Nagan, Narasimhan; Zhu, Hui; et al. (2012): „Pan-ethnic carrier screening and prenatal diagnosis for spinal muscular atrophy: clinical laboratory analysis of >72,400 specimens.“. In:

European journal of human genetics : EJHG. Nature Publishing Group 20 (1), pp. 27–32, DOI: 10.1038/ejhg.2011.134.

Sumner, Charlotte J (2006): „Therapeutics development for spinal muscular atrophy.“. In: *NeuroRx : the journal of the American Society for Experimental NeuroTherapeutics*. 3 , pp. 235–245, DOI: 10.1016/j.nurx.2006.01.010. — ISBN: 1545-5343 (Print)

Sumner, Charlotte J; Huynh, Thanh N; Markowitz, Jennifer A; et al. (2003): „Valproic acid increases SMN levels in spinal muscular atrophy patient cells.“. In: *Annals of neurology*. 54 , pp. 647–654, DOI: 10.1002/ana.10743. — ISBN: 0364-5134 (Print)r0364-5134 (Linking)

Sumner, Charlotte J; Wee, Claribel D; Warsing, Leigh C; et al. (2009): „Inhibition of myostatin does not ameliorate disease features of severe spinal muscular atrophy mice.“. In: *Human molecular genetics*. 18 , pp. 3145–3152, DOI: 10.1093/hmg/ddp253. — ISBN: 1460-2083

Swoboda, Kathryn J; Scott, Charles B; Crawford, Thomas O; et al. (2010): „SMA CARNI-VAL trial part I: double-blind, randomized, placebo-controlled trial of L-carnitine and valproic acid in spinal muscular atrophy.“. In: *PloS one*. 5 , p. e12140, DOI: 10.1371/journal.pone.0012140. — ISBN: 1932-6203

Vitte, Jérémie M; Davoult, Bénédicte; Roblot, Natacha; et al. (2004): „Deletion of murine Smn exon 7 directed to liver leads to severe defect of liver development associated with iron overload.“. In: *The American journal of pathology*. 165 , pp. 1731–1741, DOI: 10.1016/S0002-9440(10)63428-1. — ISBN: 0002-9440 (Print)r0002-9440 (Linking)

Wirth, B (2000): „An update of the mutation spectrum of the survival motor neuron gene (SMN1) in autosomal recessive spinal muscular atrophy (SMA).“. In: *Human mutation*. 15 , pp. 228–237, DOI: 10.1002/(SICI)1098-1004(200003)15:3<228::AID-HUMU3>3.0.CO;2-9. — ISBN: 1059-7794 (Print)

Wu, Xuefei; Chen, Po See; Dallas, Shannon; et al. (2008): „Histone deacetylase inhibitors up-regulate astrocyte GDNF and BDNF gene transcription and protect dopaminergic neurons.“. In: *The international journal of neuropsychopharmacology / official scientific journal of the Collegium Internationale Neuropsychopharmacologicum (CINP)*. 11 , pp. 1123–1134, DOI: 10.1017/S1461145708009024. — ISBN: 1461145708

Young, Philip J; Day, Patricia M; Zhou, Jianhua; et al. (2002): „A direct interaction between the survival motor neuron protein and p53 and its relationship to spinal muscular atrophy.“. In: *The Journal of biological chemistry*. 277 , pp. 2852–2859, DOI: 10.1074/jbc.M108769200. — ISBN: 0021-9258 (Print)

Zhang, Honglai L; Pan, Feng; Hong, Daewha; et al. (2003): „Active transport of the survival motor neuron protein and the role of exon-7 in cytoplasmic localization.“. In: *The Journal of neuroscience : the official journal of the Society for Neuroscience*. 23 , pp. 6627–6637, DOI: 23/16/6627 [pii]. — ISBN: 1529-2401 (Electronic)

Appendix I

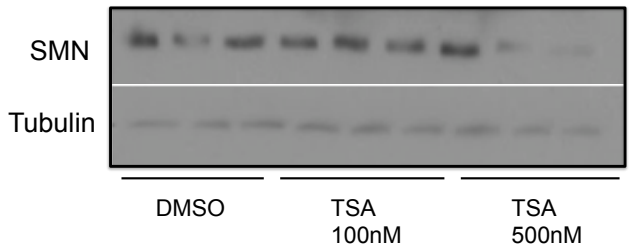

Figure A1. No changes in Smn protein levels after TSA treatment in the MEFs obtained form *Smn*$^{2B/-}$ mice.

Western blot revealed no significant increase in Smn protein levels after treatment with 100nM of TSA in SMA mice compared with DMSO controls (n=3). Furthermore there was no significant increase in Smn protein levels after treatment with 500nM of TSA in SMA mice compared with DMSO controls (n=3).

Appendix II

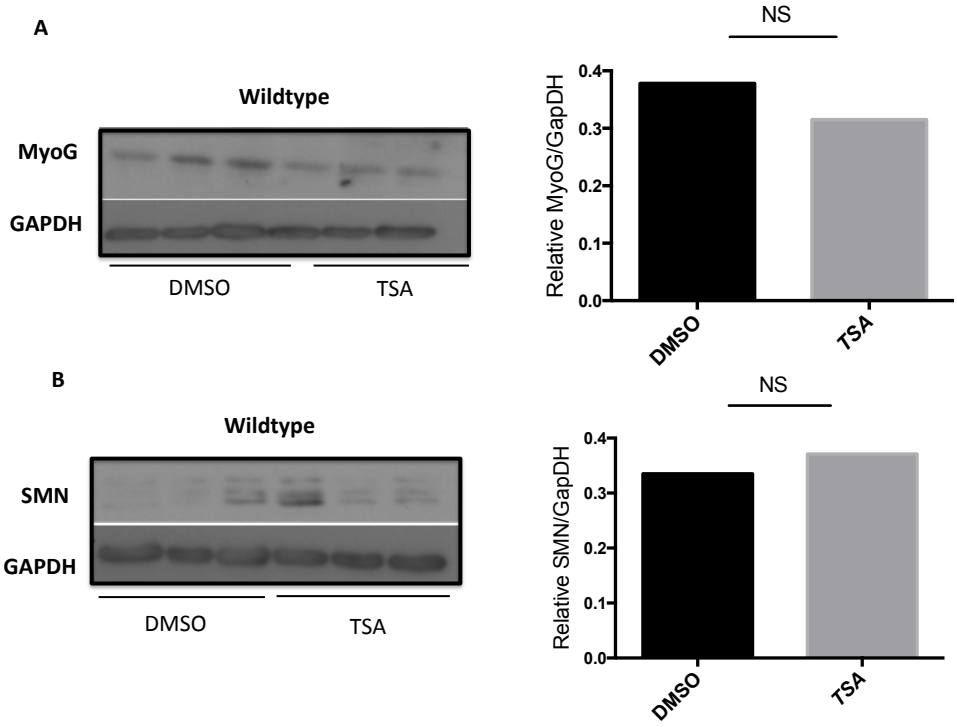

Figure A2. No change in Smn and MyoG protein levels after TSA treatment in the hind limb muscle of wildtype mice**.**

A) Western blot and quantification analysis showing that serial TSA injections do not increase MyoG levels in the hind limb muscle of P25 wildtype mice (n=3). **B)** Western blot and quantification analysis showing that serial TSA injection had no impact on Smn protein levels in hind limb muscle of P25 wildtype mice (n=3).

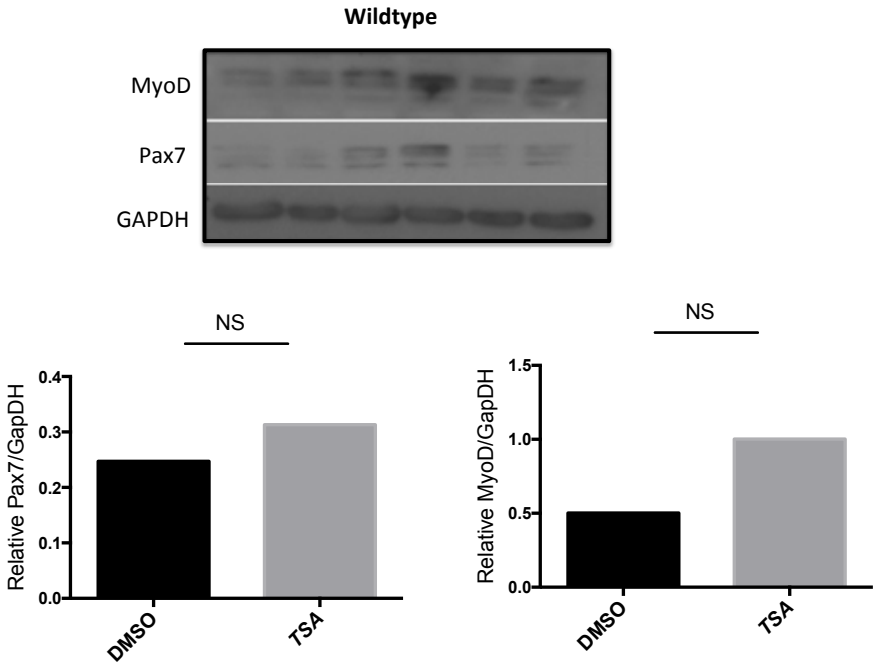

Figure A3. No change in MyoD and Pax7 protein levels after TSA treatment in the hind limb muscle of wildtype mice**.**

Western blot and quantification analysis showing that serial TSA injections do not increase MyoD and Pax7 levels in the hind limb muscle of P25 wildtype mice (n=3).